

## **Copyright Warning & Restrictions**

The copyright law of the United States (Title 17, United States Code) governs the making of photocopies or other reproductions of copyrighted material.

Under certain conditions specified in the law, libraries and archives are authorized to furnish a photocopy or other reproduction. One of these specified conditions is that the photocopy or reproduction is not to be “used for any purpose other than private study, scholarship, or research.” If a user makes a request for, or later uses, a photocopy or reproduction for purposes in excess of “fair use” that user may be liable for copyright infringement,

This institution reserves the right to refuse to accept a copying order if, in its judgment, fulfillment of the order would involve violation of copyright law.

**Please Note: The author retains the copyright while the New Jersey Institute of Technology reserves the right to distribute this thesis or dissertation**

Printing note: If you do not wish to print this page, then select “Pages from: first page # to: last page #” on the print dialog screen

The Van Houten library has removed some of the personal information and all signatures from the approval page and biographical sketches of theses and dissertations in order to protect the identity of NJIT graduates and faculty.

## ABSTRACT

Title of Thesis: A Purely Chemical Nitrogen Dioxide Laser

Conrado M. Malalis, Master of Science, 1981

Thesis directed by: Dr. Joseph W. Bozzelli, Associate  
Professor of Chemistry

Purely chemical lasers promise to provide future high-power lasers for remote installations, airplanes, ships and in space without the necessity of external electric power sources.

This study is about the design and construction of a new, gas phase purely chemical  $\text{NO}_2$  laser, based on the reaction of  $\text{NO} + \text{O}_3 \rightarrow \text{NO}_2^* + \text{O}_2$ . The vibrationally excited  $\text{NO}_2^*$  species at 1-40 mm Hg total pressure is the source of energy (photons) for the laser. A series of computer program calculations on the reaction kinetics and relaxational processes involved have also been made, showing support for the formation of a population inversion of the vibrationally excited species ( $\text{NO}_2^*$ ). The optimum kinetic parameters were determined from these calculations. Two reactor tube systems were constructed for the experiments, one shorter in length (shorter reaction time) than the other, both of which did not show consistent positive results. The maximum time needed for optimum population inversion was attainable in the experiments with the second laser reactor, but higher total concentration of

excited  $\text{NO}_2^*$  species in the activity medium are needed.

The results obtained with these two laser tube reactors and the kinetic calculations permit the design of a yet improved third generation laser assembly. The third generation laser tube, with transversial flow design as well as a fast, powerful vacuum pump, has been designed on calculations which show that lasing will be achievable.

A PURELY CHEMICAL NITROGEN  
DIOXIDE LASER

by

Conrado M. Malalis

Thesis submitted to the Faculty of the Graduate School of  
the New Jersey Institute of Technology in partial  
fulfillment of the requirements for the degree of  
Master of Science in Engineering Science (Chemistry)  
1981

Blank Page



VITA

NAME: Conrado Mendoza Malalis

PERMANENT ADDRESS:

DEGREE AND DATE TO BE CONFERRED: MS Eng. Sc. (Chemistry), 1981

DATE OF BIRTH:

PLACE OF BIRTH:

SECONDARY EDUCATION: Far Eastern University Boy's High School,  
1961

COLLEGIATE INSTITUTIONS ATTENDED	DATE	DEGREE	DATE OF DEGREE
New Jersey Institute of Technology	1974-81	MS Eng Sc (Chem)	1981
Mapua Institute of Technology	1961-67	BS ChE	1967

MAJOR: Engineering Science (Chemistry)

POSITIONS HELD: Research Chemist (1978-Present)--Mobay Chemi-  
cal Corporation, 169 W. 52nd St., Bayonne,  
New Jersey 07002

Research Chemist (1969-78)--Sun Chemical  
Corporation, 441 Tompkins Avenue, Staten  
Island, New York



## DEDICATION

This book is heartily dedicated to my wife, Carmelita, and to my two children, Christine and Carmelyn, whose love and affection I always cherish and remember.

## ACKNOWLEDGMENT

I would like to extend my many thanks to Dr. Joseph Bozzelli, my advisor on this thesis, whose patience, advice and teachings, I deeply admire, respect and honor. His efforts made possible the completion of this thesis.

My special thanks to Mr. Hindcliff for making the IR detector operate so well.

I would also like to extend my many thanks to Diana Muldrow for her time and effort in the typing of the entire manuscript.

## TABLE OF CONTENTS

Section	Page
I INTRODUCTION . . . . .	1
II EXPERIMENTAL . . . . .	14
A. The Initial Laser Tube and Accessories . . .	14
B. Experiments Using Initial Laser Tube . . . .	32
C. Modified Laser Tube . . . . .	36
D. Experiments Using the Modified Laser Tube .	51
III THEORY . . . . .	53
A. The NO <sub>2</sub> Molecule . . . . .	53
B. Reactions . . . . .	56
C. Kinetics . . . . .	59
D. Gain Calculations . . . . .	70
IV Results and Discussion . . . . .	82
A. Initial Laser Tube . . . . .	82
B. Modified Laser Tube . . . . .	85
C. Third Generation Laser . . . . .	95
V CONCLUSIONS . . . . .	98
APPENDIX I . . . . .	100
SELECTED BIBLIOGRAPHY . . . . .	104

LIST OF TABLES

Table	Page
1 The Chemical Lasers . . . . .	7
2 Initial Laser Tube Experimental Results . . . . .	35
3 Velocity Calculations Flowmeter--Matheson #601 . . . . .	37
4 NO Flowmeter Calibration . . . . .	44
5 Nitrogen to NO Conversion of Flow Rates . . . . .	46
6 Ar/O <sub>3</sub> Flowmeter Calibration . . . . .	48
7 Modified Laser Tube Experimental Results . . . . .	52
8 Summary of Programming Results, Run No. 1 to Run No. 5 . . . . .	64
9 Summary of Programming Results, Run No. 6 to Run No. 10 . . . . .	65
10 Summary of Programming Results, Run No. 11 to Run No. 15 . . . . .	66
11 $\beta$ Values for Initial and Modified Laser Tubes . . . . .	75
12 $N_2-N_1$ for Initial Laser Tube, $\beta = 0.0272 \text{ cm}^{-1}$ . . . . .	76
13 $N_2-N_1$ for Initial Laser Tube, $\beta = 0.0543 \text{ cm}^{-1}$ . . . . .	77
14 $N_2-N_1$ for Initial Laser Tube, $\beta = 0.0353 \text{ cm}^{-1}$ . . . . .	78
15 $N_2-N_1$ for Modified Laser Tube, $\beta = 0.154 \text{ cm}^{-1}$ . . . . .	79
16 $N_2-N_1$ for Modified Laser Tube, $\beta = 0.308 \text{ cm}^{-1}$ . . . . .	80
17 $N_2-N_1$ for Modified Laser Tube, $\beta = 201 \text{ cm}^{-1}$ . . . . .	81
18 Population Inversion Reaction Distance and Residence Time in a Reactor Tube . . . . .	86

## LIST OF FIGURES

Figure		Page
1	Schematic Diagram of Initial Laser Tube and Accessories . . . . .	15
2	Chopper Blade . . . . .	19
3	Bubbler Set-up . . . . .	23
4	Manometer . . . . .	23
5	Schematic Diagram of Ozonator . . . . .	28
6	Ozone Matrix Trap . . . . .	30
7	Modified Laser Tube . . . . .	39
8	NO Flowmeter Calibration . . . . .	45
9	Ar/O <sub>3</sub> Flowmeter Calibration Stainless Steel Ball as Float . . . . .	49
10	Ar/O <sub>3</sub> Flowmeter Calibration Black Glass Ball as Float . . . . .	50
11	The NO <sub>2</sub> Molecules . . . . .	54
12	The Fundamental Mode of Vibrations of the NO <sub>2</sub> Molecule . . . . .	54
13	The Fundamental Mode of Vibrations of the NO <sub>2</sub> Molecule with Energy Levels . . . . .	55
14	Time, Distance vs. NO <sub>2</sub> Formation, Excited and Ground States . . . . .	67
15	NO Concentration vs. t <sub>max</sub> . . . . .	68
16	NO Concentration vs. NO <sub>2</sub> <sup>+</sup> (max) . . . . .	69
17	Schematic Diagram of the Third Generation Laser Tube . . . . .	97

## I. INTRODUCTION

A laser is a device which is capable of emitting an intense, unique light or electromagnetic radiation. The radiation or light produced by the laser is extraordinary because it possesses certain unusual properties which are not found in ordinary or conventional forms of radiation. These properties which make laser beams unique are: extreme brightness, directionality, high degree of coherence, monochromaticity and high degree of polarization.[1] Only a brief summary of these properties will be given here.

Brightness is defined as the power per unit area of the source per unit solid angle into which the source is radiating. The sun has a brightness of  $1.5 \times 10^5$  lumens/cm<sup>2</sup> sterad.[1] Whereas a one-milliwatt helium-neon laser gives  $2.04 \times 10^7$  lumens/cm<sup>2</sup> sterad, which shows that it is a hundred times brighter than the sun[1] in the illumination of a small area. Directionality is characterized by the spread of the laser beam output called the full angle beam divergence. This is defined as twice the angle that the outer edge of the beam makes with the center of the beam.

Coherence is another important property of the laser light. In order to understand this property, we have to remember that light or radiation has both a wave and a

particulate character. Coherence is the complete correlation or predictability both in space and time between one point of the electromagnetic wave and those at any other point.

Another property of the laser light is its extraordinary monochromaticity. In Greek, this means monos (single) and chroma (color). The laser light has a very narrow spectral width. No light source, not even the laser light, is absolutely monochromatic; that is, one single frequency. The laser light is, however, far more monochromatic than conventional light sources and researchers are achieving better and better approximations of the ideal. The last property, the high degree of polarization, can be understood in terms of the wave nature of the light. This property means that the orientation of the electric field of the wave is constant with time and only the magnitude and sign of the field changing. [1]

There are four basic requirements for a laser to operate. The first requirement is an active medium, which is a collection of atoms, molecules or ions that can emit radiation as transitions from one energy level to another, either electronic, or vibration-rotation or both. The second requirement is population inversion. This condition means that for a given volume or quantity and time, the number of the active medium (excited species) present in the higher energy level (or excited state is

greater than the number of the excited species in the lower energy level (or ground state). The third requirement is a "pumping" mechanism of exciting the active medium into higher energy level thus attaining population inversion. In addition to these three requirements a fourth is the resonant cavity.<sup>[2]</sup> In order to achieve laser action in some lasers, light needs to make many passes through the active medium to stimulate emission from the excited to ground levels (amplification). Mirrors with varying reflectivities and with various modes of curvature are placed at opposite ends of a cavity serving as the terminals of the resonant cavity.

When an excited species in its excited state interacts with a photon,  $h\nu$ , stimulated emission may occur-- that the excited molecule will emit a second  $h\nu$  which joins the initial photon  $h\nu$  at the same frequency and phase thereby amplifying or doubling the photon to  $2 h\nu$ . The excited molecule is then returned to its ground state. The difference between the two energy levels (excited and ground state) corresponds to  $E_{\text{excited}} - E_{\text{ground}} = h\nu$ . The word LASER is an acronym for Light Amplification by Stimulated Emission of Radiation.

There are many different kinds of lasers, each one operating with certain spectral wavelengths, power output, % efficiency, design and mechanisms of operation, but whatever the individual differences are, they all obey or



follow the basic requirements discussed above. Some of the lasers operate in the infrared region, like the CO<sub>2</sub> laser at 10.6  $\mu\text{m}$ , some operate in the visible region like the helium-neon laser operating at 0.6328  $\mu\text{m}$ , and some operate in the ultraviolet region like the nitrogen lasers at 0.3371  $\mu\text{m}$ . Some lasers produced continuous wave operation and some are pulsed. Some lasers use gas or vapor phase active mediums. They can be composed of vapor, liquid or solid media.

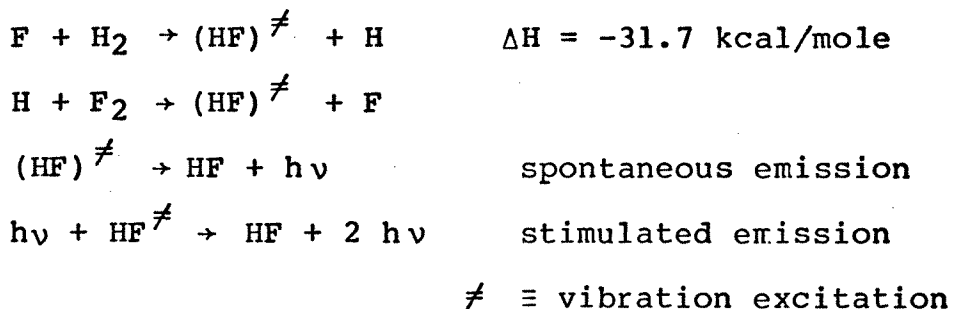
This research concerns an attempt to invent a type of laser known as gas phase purely chemical laser. Only a few examples of this type of laser are known because it is difficult to achieve population inversion entirely from chemical reaction and without the aid of external energy. The population inversion in most lasers is achieved by using energy either electrical or thermal to create extremely reactive, unstable species which will react almost instantaneously when mixed with a second reactant to produce a chemical product which exists almost solely in an excited state. The energy from a flashlamp (optical pumping) is a good example used to excite the active medium, others use discharges to dissociate stable molecules, e.g., H<sub>2</sub> to reactive atoms, H.

A purely chemical laser is a laser which utilizes its reactants in a chemical reaction to bring about population inversion without any outside energy supplied whatsoever. Most of the conventional chemical lasers are

not purely chemical because they need free atoms, i.e., H, F, Cl, Br in order to react rapidly and exothermically with the other reactant. The free atoms are provided by electrical discharge or thermally induced dissociation of species, but once the reaction has begun, additional free atoms are produced via a chain mechanism and these reactions may continue in a cycle.[2]

In the vapor phase chemical reaction of a purely chemical laser, a large amount of the energy which is released goes into the excitation of the chemical products creating the population inversion usually. The free atoms needed are generated through reactions with other reactants.

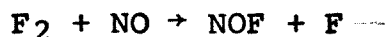
In a conventional chemical laser like the HF laser for example, the reactions involved for the lasers are:



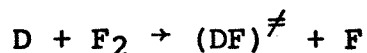
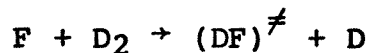
The last reaction above indicates the transition of the  $\text{HF}^{\neq}$  molecule to the lower state which is not populated by the chemical reaction. This is accompanied by emission of light energy,  $h\nu$ . The initial photon emitted can be used to effect stimulated emission (further emission) by interaction with the excited molecule in the resonant cavity.

The population inversion is produced whenever the reaction yields only excited state molecules as the end product. Some of the chemical lasers known are listed in Table 1, with their chemical reactants, reactions, lasing molecules, operating wavelengths, output power and efficiency. [3]

The first purely chemical laser made was the DF-CO<sub>2</sub> laser. [4] The source of the free fluorine atoms is provided by mixing nitric oxide with a flowing mixture of fluorine and helium as a result of the reaction



The combined flows are then rapidly mixed with deuterium and carbon dioxide to produce vibrationally excited DF via the chain branching mechanism



followed by the intermolecular transfer of vibrational, rotational energy from DF to CO<sub>2</sub>,



A continuous wave operation at 10.6  $\mu$  and a maximum power output of 0.23 w was observed. [4]

Other purely chemical lasers have been reported; these are the HF-CO<sub>2</sub>, [5] HCl, [6] HBr [7] and the CO [8] lasers. The purely chemical HF-CO<sub>2</sub> laser was achieved by employing the same analogy with the DF-CO<sub>2</sub> system. [4] A continuous wave laser operation at 10.6  $\mu\text{m}$  and a maximum power output

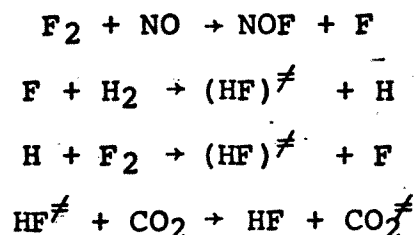
TABLE 1  
Chemical Lasers

<u>Chemical Reactants</u>	<u>Reactions</u>	<u>Laser Molecule</u>	<u>Wavelengths (<math>\mu\text{m}</math>)</u>	<u>Reported Output</u>	<u>Chemical Efficiency</u>
$\text{H}_2\text{-F}_2$	$\text{F} + \text{H}_2 \rightarrow \text{HF}^\neq + \text{H}$	HF	2.6-3.6	4500 W cw 2300 J/pulse	10
	$\text{H} + \text{F}_2 \rightarrow \text{HF}^\neq + \text{F}$				
$\text{D}_2\text{-F}_2$	Similar to HF system	DF	3.6-5.0	--	--
$\text{H}_2\text{-Cl}_2$	Similar to HF system	HCl	3.5-4.1	--	--
$\text{CS}_2\text{-O}_2$	$\text{O} + \text{CS}_2 \rightarrow \text{CS} + \text{SO}$	CO	4.9-5.7	25 W cw	2.5
	$\text{SO} + \text{O}_2 \rightarrow \text{SO}_2 + \text{O}$				
	$\text{O} + \text{CS} \rightarrow \text{CO}^\neq + \text{S}$				
	$\text{S} + \text{O}_2 \rightarrow \text{SO} + \text{O}$				
$\text{D}_2\text{-F}_2\text{-CO}_2$	$\text{F} + \text{D}_2 \rightarrow \text{DF}^\neq + \text{D}$	$\text{CO}_2$	10.6	560 W cw	5
	$\text{D} + \text{F}_2 \rightarrow \text{DF}^\neq + \text{F}$				
	$\text{DF}^\neq + \text{CO}_2 \rightarrow \text{DF} + \text{CO}_2^\neq$				
$\text{C}_3\text{F}_7\text{I}$	$\text{C}_3\text{F}_7\text{I} \rightarrow \text{C}_3\text{F}_7 + \text{I}^*$	I	1.32	65 J/pulse 1.2 GW peak	--

$\neq$  Represents vibrational excitation

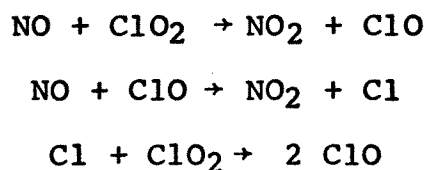
\* Represents electronic excitation

of 0.8 w was observed from the following reactions:

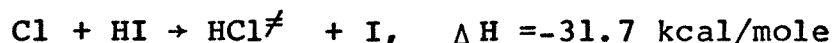


The purely chemical transverse flow HCl laser was reported having a multiline output power of 13 w and a chemical efficiency of 8%. [6]

The production of Cl atoms for an HCl laser was achieved by the following reactions: [6]

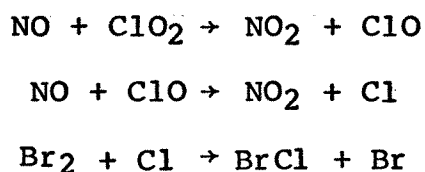


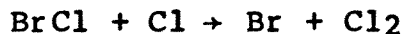
The reaction for lasing was the equation



where 70% of the reaction exothermicity appears as vibrational energy. [9] The same principle was applied successfully in a purely chemical HCl-CO<sub>2</sub> laser. [10]

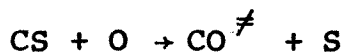
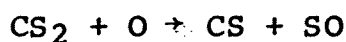
A purely chemical HBr laser was obtained in a similar manner to the purely chemical HCl laser. [7] The chlorine atoms in this laser which had been produced by the reaction of NO with ClO<sub>2</sub> were reacted with molecular bromine to form bromine atoms which, in turn, reacted with HI to form vibrationally excited HBr:





About 50-60% of the exothermicity of the last reaction appears as vibrational energy. [9] Multiline HBr output power of 0.58 w was obtained.

A purely chemical CO laser was reported utilizing combustion-generated reactants, [8] which operated from the reaction sequence



There was some difficulty in obtaining large quantities of atomic oxygen for the first reaction. This difficulty was overcome using a combustor generated technique. The combustor is fueled with  $\text{NF}_3\text{-CH}_4\text{-H}_2\text{-CS}_2$  and produces CS and S and the side products HF and  $\text{N}_2$ . [11] A supersonic expansion mixing nozzle is used to extract the CS and S from the combustor and mix  $\text{O}_2$  and diluent ( $\text{N}_2$  or He) into the flow stream. A chain reaction between CS and  $\text{O}_2$  in the mixed flow stream, initiated by S atoms, produces vibrationally excited CO. [12,13] The maximum power obtained was 700 mW operating with He in a free expansion.

Purely chemical lasers promise to provide future high-power lasers for remote installations, e.g. in airplanes, ships and space, without the necessity of electrical power as required in other conventional lasers.

This study was an attempt to make a purely chemical

NO<sub>2</sub> laser from the reaction of NO with ozone,  $\Delta H = -48$  kcal/mole. [14,15] No such laser had been reported that described the reaction and exothermicities of producing the vibrationally excited NO<sub>2</sub><sup>\*</sup> molecule. The probability of lasing due to a population inversion of NO<sub>2</sub><sup>\*</sup> probable as indicated by the following studies made of the NO<sub>2</sub> molecule.

In the early 60's, A. Fontijn, C.B. Meyer and H.I. Schiff were among the first investigators to report the spectral distribution of the chemiluminescent reaction  $O + NO \rightarrow NO_2^* + h\nu$  from 3875 Å to 14,000 Å wavelength region. [16]

P.N. Clough and B.A. Thrush later conducted vibrational emission studies of the reaction  $O_3 + NO \rightarrow NO_2^* + NO_2^{\neq} + O_2 + 48$  kcal/mole. [15,17] They reported that about 93% of the NO<sub>2</sub> is formed in the ground state and 7% in the electronic state. M.F. Golde and F. Kaufman studied also the vibrational emission of NO<sub>2</sub> from the same reaction and found that a large percentage of the NO<sub>2</sub> produced by the reaction was, in fact, vibrationally excited. [18] This conflicted with Clough and Thrush's conclusions. A.E. Redpath and M. Menzinger, using seeded supersonic NO beams studied the electronic (NO<sub>2</sub><sup>\*</sup>) and vibrational (NO<sub>2</sub><sup>‡</sup>) chemiluminescence of the NO + O<sub>3</sub> reaction. They concluded that a large percentage of NO<sub>2</sub> produced was indeed vibrationally excited, as predicted by Golde and Kaufman and that proved Clough and Thrush's conclusion to be in error. Therefore population inversion is probable in

the reaction, and can be utilized to make a purely chemical laser from the reaction of  $\text{NO} + \text{O}_3$ . In addition, Clough and Thrush also reported the vibrational emissions from the reaction to be in the 3.4-3.8  $\mu\text{m}$ , relatively intense, a second weaker band between 2.4 and 2.6  $\mu\text{m}$  which could only be observed at high resolution and a third band between 6 and 7.25  $\mu\text{m}$  with a peak at 6.2  $\mu\text{m}$ , which is relatively intense and a fundamental mode of vibration. [17] Golde and Kaufman found that the vibrational emission between 3.2  $\mu\text{m}$  and 4.0  $\mu\text{m}$  region centering at 3.6  $\mu\text{m}$ . [18] E. Bar-Zin, J. May and R.J. Gordon studied the reaction over the temperature range 158-437 $^\circ\text{K}$  using a  $\text{CO}_2$  TEA laser to excite vibrationally the ozone and found that the total decay rate of the laser-induced chemiluminescent signal showed a strong non-Arrhenius temperature dependence. [19] K.K. Hui and T.A. Cool made studies of the laser-enhanced reaction between the vibrationally excited  $\text{O}_3$  and  $\text{NO}$  and found that the stretching and bending modes of  $\text{O}_3$  make comparable contributions to reaction state enhancement. [20]

In this research work, we used initially a long glass tube as our reactor for the reaction of  $\text{NO} + \text{O}_3$  (initial laser tube). The  $\text{NO}$  was premixed with Argon in a round 1 liter flask prior to reaction with  $\text{O}_3$ . The  $\text{O}_3$  was generated by an ozonizer through an oxygen feed and the ozone was made to pass through a silica gel contraption (ozone matrix trap) at cryogenic temperature ( $-80^\circ\text{C}$ ) under a blanket of argon.



Argon was also used to carry the ozone into the laser tube. Two sodium chloride discs served as windows for the laser tube. Two gold coated mirrors, one concave (100% reflectance) and the other flat and having a small aperture (97-98% reflectance) were used for the resonant cavity operation. The infrared radiation coming out of the laser tube was chopped by an aluminum chopper, detected by a pyroelectric detector and then displayed in an oscilloscope. A reference light chopped by the same chopper, detected by a solar cell and displayed in the same oscilloscope was also used for comparison with the laser IR radiation. A vacuum pump served to draw the product, reactants and other species out from the laser tube in a steady and continuous operation. A bubbler was used to keep the  $O_3$  trap at 1 atm plus 1 to 2 cm of oil pressure and prevent any sudden changes of pressure. A manometer was used to monitor the total pressure in the system. Several runs with different mixtures of NO with Argon were tried, but the oscilloscope readings were very erratic and inconclusive. A computer programming of the kinetics of the reactions involved was formulated, and the population inversion was calculated, printed out and evaluated with time variations. It appeared that the optimum time for maximum population inversion required a smaller laser tube. A smaller laser tube was made (modified laser tube). Other modifications were introduced, among them were the NO and Ar/ $O_3$  flow meters.

The IR detector was rebuilt and showed better sensitivity. All the experiments from both laser tubes were recorded, analyzed, and concluded. The same was done with the results of the computer programming print out. Gain calculations were also made to see whether the required minimum population inversion is likely to occur in both laser tubes.

A much detailed picture of the undertakings of this research study can be found in the coming sections.

## II. EXPERIMENTAL

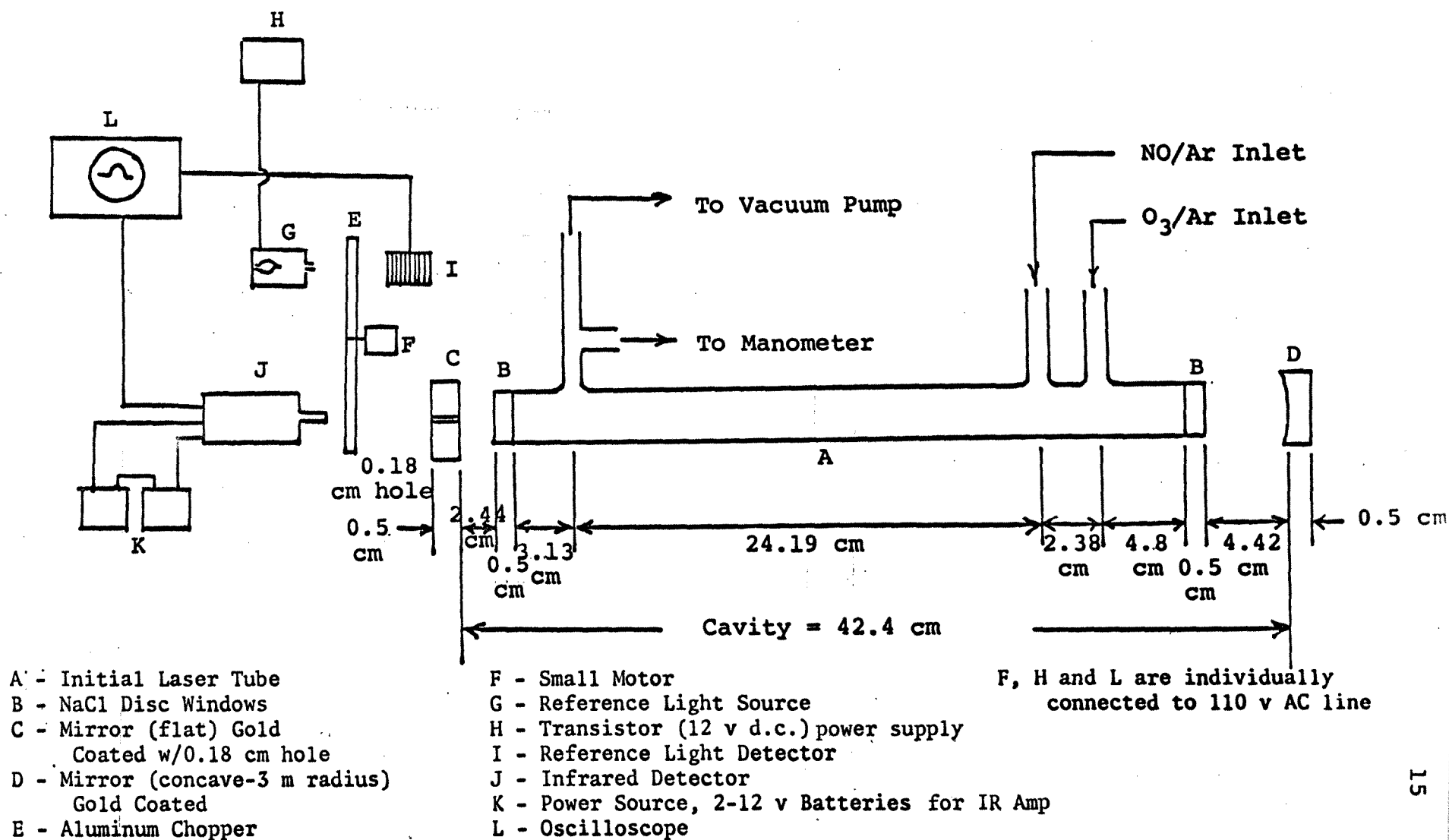
### A. The Initial Laser Tube and Accessories

1. Initial Laser Tube--The initial laser tube used was a Pyrex glass tube and is illustrated in Figure 1. It had an internal diameter of 2.18 cm and a length of 34.5 cm. A small inlet tube with an outside diameter of 1.3 cm was located 4.8 cm away from one of the ends of the tubing. This served as the inlet for the ozone and argon gases. A second small tube with an internal diameter of 0.5 cm was located on the same side 2.38 cm away from the ozone/argon inlet. This NO gas inlet was 7.18 cm farther away from the same end. An outlet tube with an internal diameter of 1.0 cm was located near the other end of the laser tube. This tubing, which was 3.13 cm away from the outlet mirror end, and 24.2 cm from the NO inlet. It connected to a vacuum pump and was the outlet for the products of the reaction, unreacted reactants and argon or other carrier gas.

Two identical sodium chloride (NaCl) disc windows, 25.2 mm in diameter and 5.0 mm thick, were mounted on the ends of the tube with silicon adhesive.

2. Cavity--A resonant cavity is one requirement of a vapor phase laser. It is a geometrical structure, with two parallel mirrors placed a known distance apart with the laser tube between. [2] The active medium is usually in the center of the resonant cavity within the glass in this case. The light produced by the active medium travels

Fig. 1 Schematic Diagram of Initial Laser Tube and Accessories



back and forth between the mirrors and it is amplified via stimulated emission from the lasing species on each pass in the medium. One of the mirrors is usually 100% reflecting while the other passes a small percentage of the light, allowing the laser light to be output or detected.

In this experiment, the resonant cavity consisted of two mirrors which were 42.4 cm apart. The mirrors were made of glass with diameters of 3.2 cm and a thickness of 0.6 cm. A very thin coating of gold on the surface was applied to have maximum reflectance. The first mirror was concave with a 3 meter radius of curvature and 100% reflectance. The other mirror was flat and had a small opening of 0.18 cm diameter at the center to allow the laser output radiation. Calculations using the values of the diameters of the hole and of the laser tube showed that the flat mirror had 97.6% reflectance:

$$\begin{aligned}
 \% \text{ Reflectance} &= \frac{\text{cross-sectional area of laser tube} - \text{area of hole}}{\text{cross-sectional area of laser tube}} \\
 &\times \text{reflectance of Au in IR} \times 100\% \\
 &= \frac{\pi \left[ \left( \frac{2.18}{2} \right)^2 - \left( \frac{0.18}{2} \right)^2 \right]}{\pi \left( \frac{2.18}{2} \right)^2} \times 0.983 \times 100\% \\
 &= \frac{1.1881 - .0081}{1.1881} \times 0.983 \times 100\% \\
 &= 0.993 \times 0.983 \times 100\% \\
 &= 97.6\%
 \end{aligned}$$

This laser cavity design using one flat mirror and one concave with radius of curvature greater than the distance between them helped to confine the beam in the cavity of the laser tube. The stability condition established for optical resonators was,

$$0 < g_1 g_2 < 1$$

where,  $g_1$  and  $g_2$  are the g-parameters and are defined by the equations

$$g_1 = 1 - \frac{L}{r_1}$$

and

$$g_2 = 1 - \frac{L}{r_2}$$

where  $r_1$ ,  $r_2$  were the radii of curvature of the mirrors, 300 cm for the concave mirror and  $\infty$  for the flat type.  $L$  is the distance between the two mirrors, 42.4 cm. Substituting the values of  $r_1$ ,  $r_2$  and  $L$  showed  $g_1 = 0.8587$ ,  $g_2 = 1$  and so the product  $g_1 g_2$  gave us 0.8587 which was within the range called for by  $0 < g_1 g_2 < 1$  condition implying a stable condition existed in the laser cavity.<sup>[21]</sup> See Figure 1 for the diagram of the resonant cavity.

3. Infrared Laser Light Detector--The infrared (IR) light which should be lasing out from the resonant cavity was to be chopped at a 13.98 Hz with a 6 aperture chopper rotating at 2.33 Hz and monitored by a pyroelectric detector,

preamplified, amplified and the AC wave form displayed into the oscilloscope. It could also be input to a lock-in amplifier for detection.

This detector, Model LCP-200T<sup>[22]</sup> was used for chopped radiation systems, has a broad spectral response 321 volt/watt, detectivity ( $D^*$ ) of  $0.8 \times 10^8$  cm-Hz<sup>1/2</sup>/watt and noise equivalent power (NEP) of  $1.5 \times 10^{-9}$  watts/Hz<sup>1/2</sup>. The ambient temperature range was -20 to 80°C. Tests on the detector showed that it met the specifications. The detector had a Germanium window with spectral transmission between 1.8 and 500 microns and was housed and enclosed in a small cylindrical metal box with a round opening of diameter 0.32 cm through which the infrared radiation entered. The aperture was about 0.30 cm in height and had four leads leading to the amplifier, and detection operational circuitry.

4. Chopper--The chopper was made of thin, circular aluminum sheet with an outside diameter of 15.2 cm. It was divided into exactly twelve sections and each section occluded an angle of 30°. Six of the sections were cut out and located in alternate positions with the other six which were not cut out. A diagram of the chopper is shown in Figure 2.

A hole was provided in the middle of the chopper for connection to the shaft of a small motor needed to rotate the chopper. This motor was powered by a 110 V AC line.

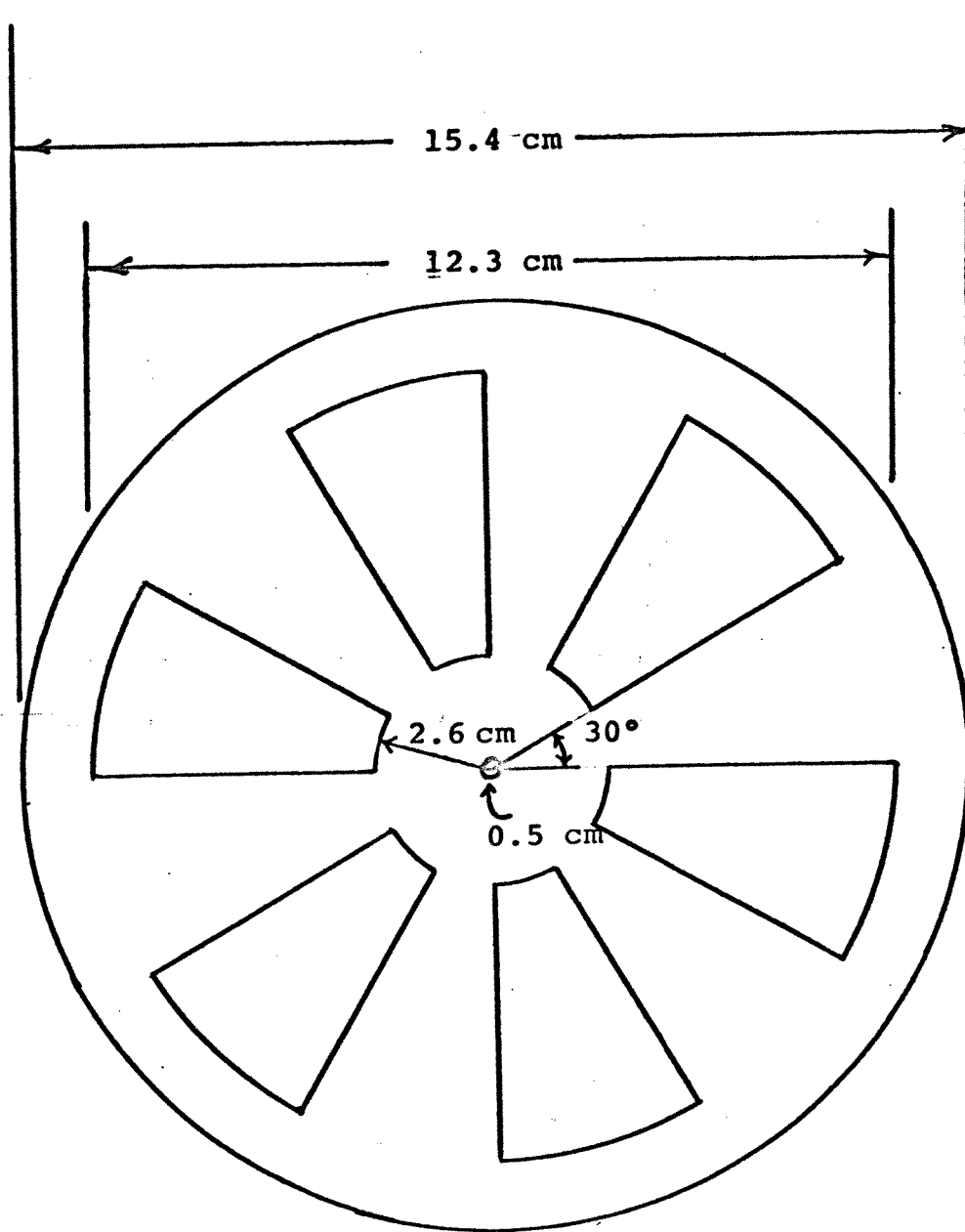


Fig. 2 Chopper Blade



A switch was used to turn it on and off.

The shaft revolved at 140 rpm, or 2.33 revolutions per second. Each shaft revolution included the 12 sections or 6 on/off cycles yielding a chopping frequency of 13.98 Hz. By subjecting the reference light (see section 5) and the laser radiation coming from the laser tube to this on/off (chopped AC) operation, the detection of laser signal could be performed at optimum sensitivity.

5. Reference Light and Reference Light Detector--The source of the reference light was a 12 volt DC auto bulb (#53 Lamp Heavy Duty by Sylvania) with a tungsten filament. The bulb was enclosed in a small metal box completely sealed in from the outside. A small round opening served as the outlet for the light.

The power supply to bulb was from a 12 V DC power supply connected to 110 volt AC line. This transistor power supply was equipped with rectifier and was connected to the reference light source in order to convert the line AC to DC current reduced the output voltage down to 12 volts. AC operation of the reference lamp would have given a large 60 cycle signal to reference detector.

A solar cell was used to detect the reference light. It was a small rectangular piece 3 cm by 2 cm with connectors that led to the oscilloscope and reference signal of the lock amplifier. See Figure 1 for the diagram of the set up. The solar cell was purchased at Radio Shack.

6. Vacuum Pump--The NO, O<sub>3</sub> and argon gases were admitted into the laser tube in a continuous flow during the experiment in order to produce a steady state reactor system. The products, NO<sub>2</sub>, O<sub>2</sub> and the unreacted gases, NO and O<sub>3</sub>, plus argon and other possible products were drawn out of the system in a continuous manner by the vacuum pump, Model 1402, W. M. Welch Manufacturing Company with an operating speed of 525 rpm. The flow rate of vapor removed from the system affected the results by having varied the time reactants and products spent in the cavity and the total pressure. This is discussed in detail in Section IV, Results and Discussion.

The vacuum pump used was attached to the outlet tubing of the laser tube, and had a capacity of 205 liters/min.

7. The Bubbler System--The bubbler system (see Figure 3) was composed of a vent tube from the ozone/NO/argon inlet system leading into a test tube partially filled with oil to act as an isolation and relief valve to prevent pressure or vacuum surges on the condensed ozone. This tube was partly filled with silicone oil to a height of 3.5 cm. The open end of a longer vent tube was immersed 1.0 cm under the silicone oil. This vent tube was connected to a T-shaped stopcock (3-way inlet or outlet) which led to the argon and ozone gas lines and ozone trap.

The 3-way stopcock allowed the argon gas coming from the cylinder tank to flow partially into the laser tube

while a small percentage (excess) bubbled through the silicone oil out into the atmosphere. This maintained the system leading to the needle valve at  $1 \text{ atm} \pm 1.5 \text{ cm oil}$  ( $0.001 \text{ atm}$ ). It also prevented any sudden changes of pressure on the liquid ozone. A flow of the argon was always input to the laser system tube (in addition to that of the bubbler excess) to prevent any backflow of the  $\text{NO}$ ,  $\text{O}_3$  and  $\text{NO}_2$  from the silicone oil out to the atmosphere.

A visual observation of the bubbling rate, argon venting through the bubbler, helped to determine any need for readjustments of the argon gas flow rate, especially during and after ozone production and inlet to the laser cavity. Besides the bubbler, keeping an eye to the manometer (see Section 8) reading was important to monitor the actual pressure changes brought about by the flow and interaction of the different gases.

8. Manometer--A U-shaped glass tube with an outside diameter of 0.9 cm and a height of 48.5 cm was used as the manometer, see Figure 4. It was filled with 26.5 cm of silicone oil, density of 0.884 g/cc. A stopcock at the top of each sidearm served to open or isolate each arm. This then connected to a single tubing which in turn led to the exhaust line of the laser tube.

When both stopcocks were open, no difference in height between the two sidearms were visible. When either one of

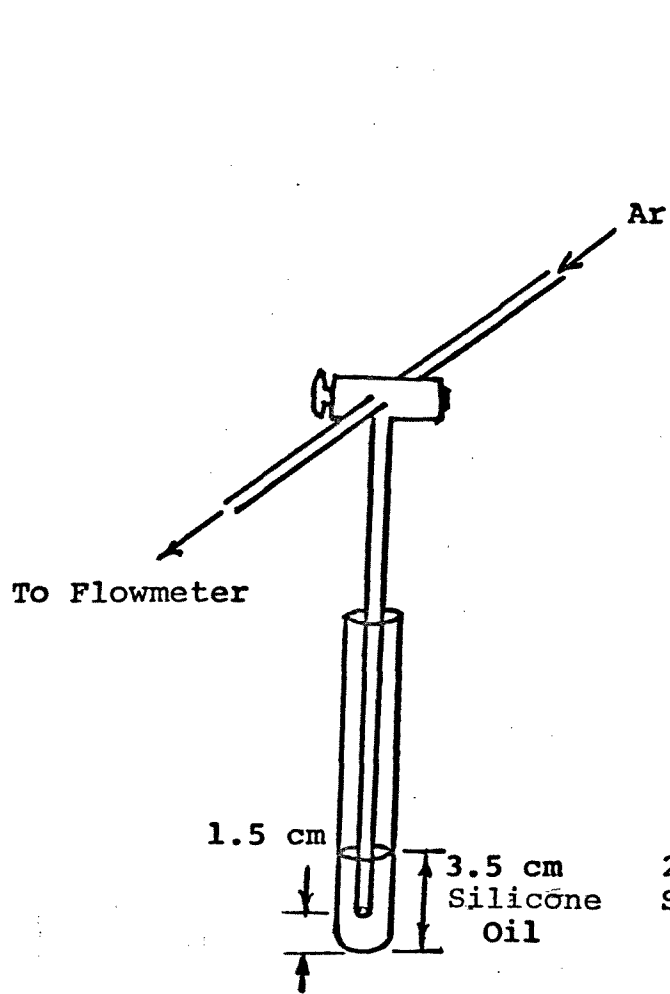


Fig. 3  
Bubbler Set-Up

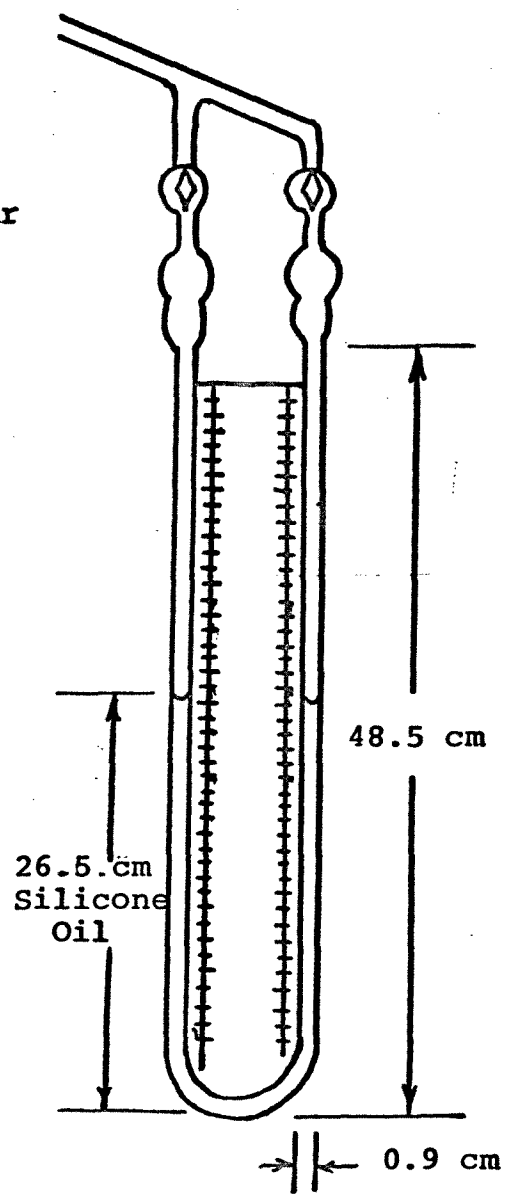


Fig. 4  
Manometer

the sidearm was closed and the other opened to the laser cavity a difference in height of the silicone oil in the sidearm indicated pressure in the tube. This difference in height, read in centimeters  $0.64 = (0.864/13.6) \times 10$  cm/mm of oil, multiplied by the factor 0.64 (for 1 cm of oil = 0.64 torr) will give the total pressure of the system.

When the inlets of NO and O<sub>3</sub> were closed and the vacuum pump was running, the pressure obtained was that of the system. As NO and O<sub>3</sub>/Argon were fed into the system, the pressure reading varied according to the flows.

9. Nitric Oxide, NO--Nitric oxide (NO) gas (compressed) was contained in a small cylinder and had 98% purity as purchased from Matheson Co., Rutherford, N.J. It was used without further purification.

The NO gas passed from the cylinder to a gas inlet manifold where one outlet led to a 1 liter round bottom flask. The flask was wrapped by a wire screen for protection purposes against explosion and was supported by an iron ring with rubber cushions.

It was in this flask where the desired amounts of NO and Ar gases were premixed prior to its reaction with the ozone inside the laser tube. This was done by evacuating the flask, admitting 7 cm Hg pressure of NO and then filling the flask to 1 atm with Argon, to make a  $7/76 \times 100\% =$

### 9.2% NO in argon mixture.

A pressure gauge calibrated in cm Hg connected to the manifold monitored the amounts of NO and Ar which were in the flask. Using the ideal gas law  $PV = nRT$ , the number of molecules of the mixture of NO and argon gases were determined.

A needle valve located between the flask and the laser tube was then used to regulate the flow of the NO/Ar mixture into the laser tube.

10. Argon and Oxygen--Argon gas was obtained from a compressed gas cylinder (Liquid Carbonic) and had a purity of 99.99%. It was used without further purification.

Argon was used to prevent any backflow of the ozone formed in the ozonator into the atmosphere during the process of making ozone and storing it in the cryogenic trap and as a carrier gas. To accomplish this, the flow rate of argon was properly adjusted so that some extra argon was always passing through the bubbler, in addition to flow over the ozone trap into the vacuum line keeping an argon blanket over the ozone.

After the ozone production, argon function shifted from preventing backflow of ozone to carrier of ozone into the laser tube. Ozone was always under an atmospheric blanket of argon. Argon was kept flowing through the system from the start of the ozonation, during and after

the reaction of NO and O<sub>3</sub> into the system. Excess argon was permitted to escape through the bubbler out to the atmosphere. The flow rate was sometime vigorous, depending upon the requirement of the existing condition in the system, and together with the bubbler constituted a safety valve for the liquid adsorbed ozone.

Oxygen was obtained for input to the ozonator from compressed gas cylinders (Liquid Carbonic Co.). A purity of 99.9% was used without further purification.

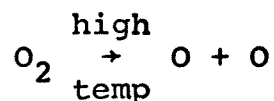
When ozone was completely deposited in the trap, see section 11, the by-pass was opened and the flow rate of oxygen was then gradually reduced to zero. At the same time, the flow rate of argon was being properly adjusted to compensate pressure and keep Ar blanket over the ozone trap.

11. Ozone and Ozonator--Ozone (O<sub>3</sub>) gas which was used in the initial laser experiments was made using an ozonator (by Welshbach Corp. Style T-23, 115 V, 1.2 amp).

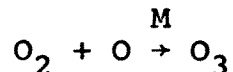
Oxygen at 99.9% purity (Matheson) compressed in a cylindrical tank was allowed to flow at a pressure of 4.5 psi and flow rate of 0.04 to 0.2 std. cubic feet per minute (1.132 to 5.66 liters per minute) into the ozonator.

The basic ozonation process occurring in the ozonator was carried out in a tube where the oxygen gas was flowing. Inside this tube was a high temperature wire

heated by current from a 0 to 120 volt supply. In this case, the potential was set at 100 volts for a period of 5 to 6 minutes. During this event, the oxygen gas near the wire dissociates into atomic oxygen:



The atomic oxygen recombined with the other oxygen molecules to form ozone gas according to the equation:



The tube which contained the high temperature wire was, in turn, inside another tube where cooling water continuously ran, to dissipate excess heat from the tube. The conversion of the oxygen to ozone was only fractional in the ozonizer and ozone gas product was mixed with unreacted oxygen. The mixture of gases goes into the ozone matrix trap. See Figure 5 for the schematic diagram of the ozonation process.

12. Ozone Matrix Trap--The ozone produced in the ozonation process will be used at a given period of time for the reaction with NO gas. The storing of a small amount of ozone without oxygen was essential in order to regulate the flow of the gas to the laser tube and limit the deexcitation of the lasing species by O<sub>2</sub>. Since ozone is considered to be reactive and somewhat unstable, only enough ozone to conduct the experiments within safety limits was pro-



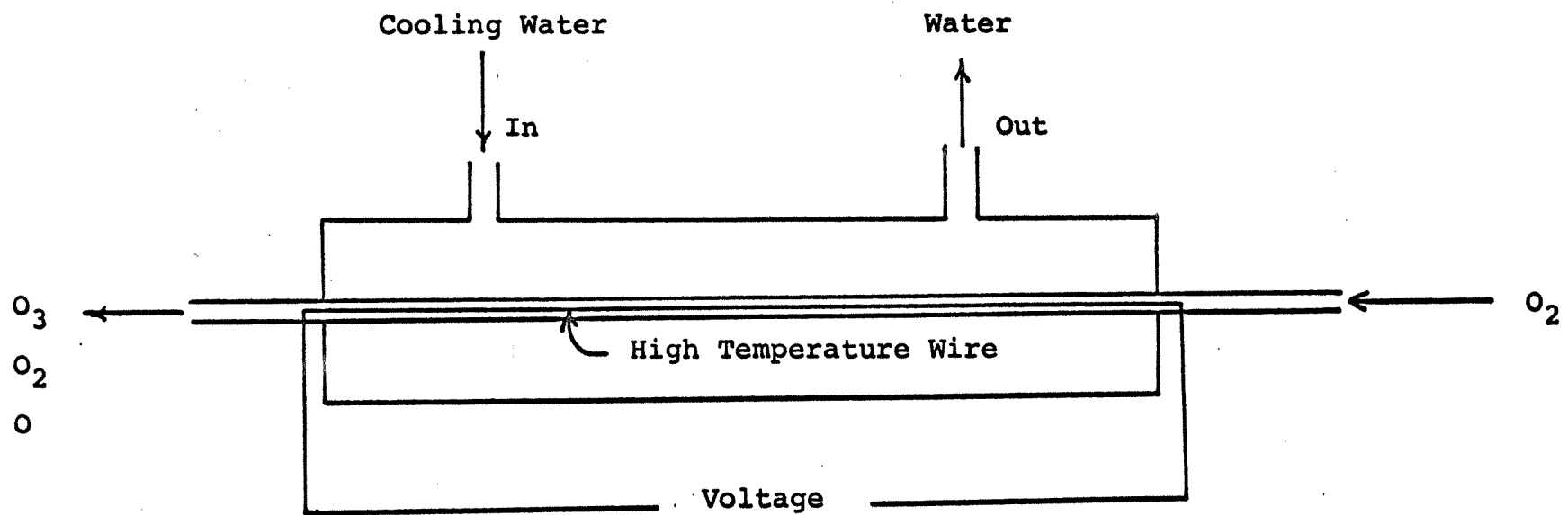


Fig. 5 Schematic Diagram of Ozonator

duced in the ozonation process.

In order to store the pure ozone, an ozone matrix trap was employed at cryogenic temperature ( $-80^{\circ}\text{C}$ ), see Figure 6. The trap itself was a tube of outside diameter 2.5 cm and 19.5 cm in length, filled with 6 cm of silica gel with a ground glass joint lubricated with halocarbon stopcock grease. A long glass tubing of outside diameter of 0.82 cm was immersed in the silica gel. This tubing was the outlet of the ozone coming from the ozonator, the top portion was outlet to the laser tube. A by-pass tubing of the same diameter, 0.82 cm, containing a stopcock was part of the system. The stopcock was kept closed during ozonation and opened only when desired to bypass the ozone trapped in the test tube.

In order to trap ozone into the matrix, the temperature must be sufficiently low, at cryogenic temperature of  $-80^{\circ}\text{C}$  to adsorb  $\text{O}_3$  onto the surface of silica gel beads. At this temperature ozone gas turned into liquid on the surface of the silica gel and could be seen to be adsorbed in silica gel by its strong blue color.

A dewar with an internal diameter of 6.8 cm, half filled with methanol was precooled to cryogenic temperature ( $-80^{\circ}\text{C}$ ) using a cryogenic apparatus (Cryo Cool CC-80f by Neslab Instruments) for 30 to 45 minutes. After this period, the temperature of the methanol in the dewar goes

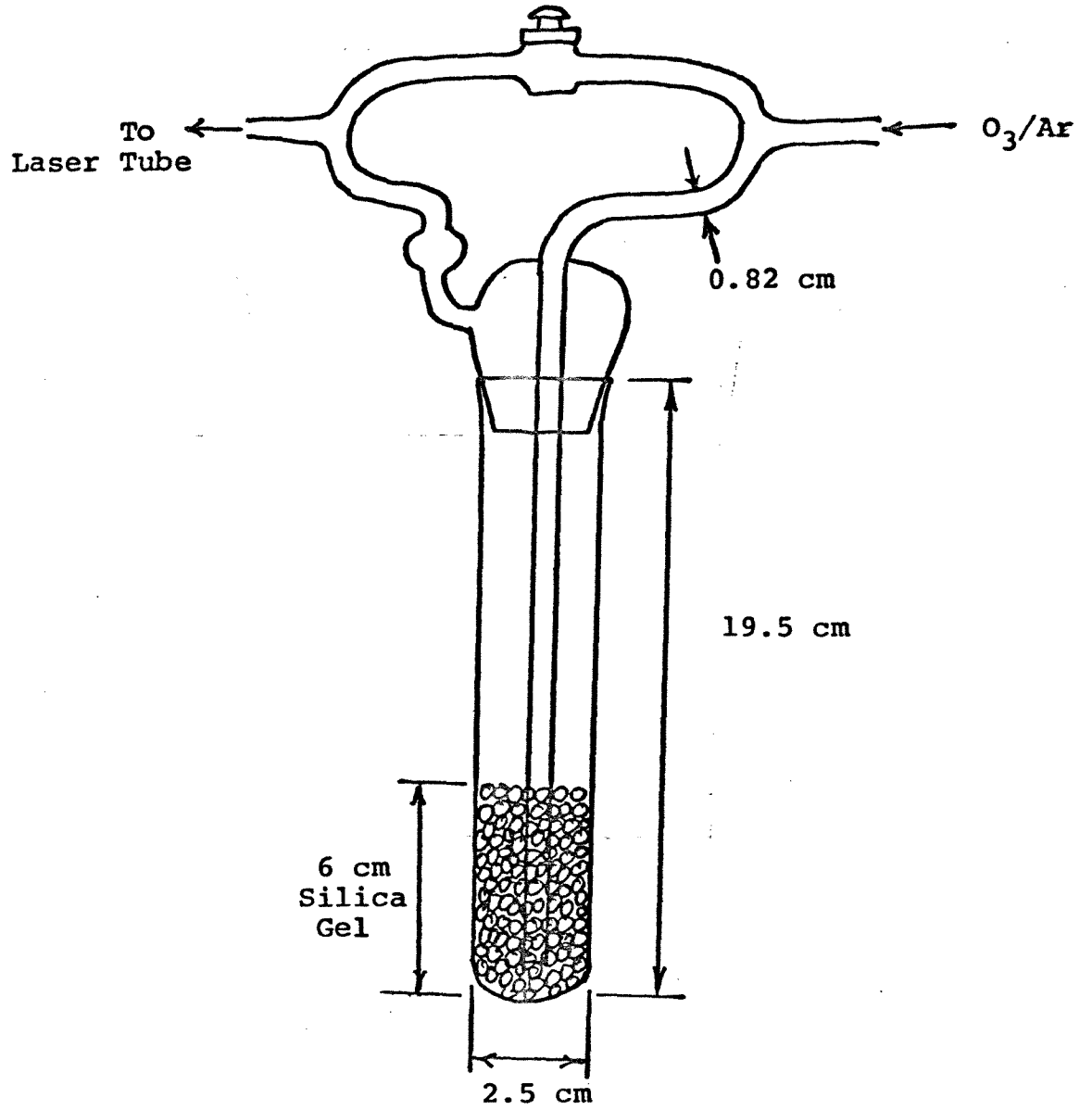


Fig. 6 Ozone Matrix Trap

down to  $-80^{\circ}\text{C}$ , as monitored with an ammonia thermometer. The ozone trap was then immersed in this dewar during the entire ozonation process, exhausting the  $\text{O}_2$  out to the vacuum pump.

When ozonation ceased, the dewar remained in the trap, the bypass line was opened to allow argon gas to pass through without the ozone. At the time the experimentation was to commence, the dewar was removed from the ozone matrix trap, the bypass line closed and argon was passed through the matrix. This allowed the argon to sweep a fraction of the ozone out and into the laser reaction tube. Here it reacted with NO to form the excited  $\text{NO}_2^*$ .

## B. Experiments Using Initial Laser Tube

The early studies were conducted using the initial laser tube, with the apparatus set up as shown in Figure 1.

The heart of the system was the laser tube and cavity. When the main reactants NO and O<sub>3</sub> combined and produced NO<sub>2</sub> which was constantly being produced and removed together with the other species present (argon, O<sub>3</sub>, NO and O<sub>2</sub>) to a vacuum pump (steady state reactor). The functions of each component of the apparatus in the system was discussed in depth in the previous sections. It is the purpose here to show how these components fitted together as an integral part of the experiment.

The vacuum pump was turned on at the start of an experimental run. Then, with the pump on, the laser tube and manometer were evacuated by opening the big stopcock that served to connect the vacuum pump to the laser tube, manometer and to other parts of the system with all the needle-valves of NO and O<sub>3</sub>/argon in a closed position. Evacuation time of the laser tube, as well as the manometer, was carried out for times of 10-15 minutes to ensure all trap gases were evacuated from the system and that it was operating properly. During this time, the NO gas was mixed with argon gas in the round bottom flask. This was done by using an auxilliary pump which could be monitored by a vacuum up to -76 cm Hg gauge. As the round bottom flask

was filled with NO gas coming from the compressed gas cylinder through the gas manifold, all stopcocks leading to the laser tube, from argon cylinder were closed. The argon gas was then admitted and just like before, all the stopcocks were closed except that of the argon line. The whole operation took several minutes. The round bottom flask was closed after the desired mixture of NO and argon was obtained and remained closed until the ozone gas was ready for reaction.

Pure argon gas was then allowed to pass directly to the bubbler and then to the laser tube and out the pump. At this time, the manometer also registered the pressure which is 5.7 cm of oil or 3.65 torr (1 cm oil = 0.64 torr). During the ozonation process, we used 0.020 std cubic feet per minute of oxygen at 100 V for six minutes. All ozone used in all experiments was made in these parameters. The manometer reading when both argon and ozonation process is in progress, was 10 cm of oil or 6.4 torr. The generated ozone was trapped into the ozone matrix trap.

After the ozone was stored in the trap, the ozonizer power was turned off and the flow rate of oxygen was gradually reduced to zero. The flow rate of argon was regulated to maintain a pressure sufficient to keep excess argon passing through the bubbler. The bubbling of argon in the bubbler was a good indication that the argon bath

in the system was properly maintained.

The reaction of the NO with  $O_3$  in the laser tube started by removing the dewar from the ozone trap, closing the bypass, thus allowing argon to pass through the trap, picking up and mixing with ozone as it flowed to the laser cavity tube. The NO/Ar mixture was thus inlet into the laser tube.

Several experimental runs were made, the variations were mainly the ratio of the NO with argon from the round bottom flask keeping all the parameters constant. See Table 2 for the variation and results. Unfortunately, none of the combinations given showed strong lasing. Weak indications of lasing were periodically observed, but the results were not consistently reproducible.

TABLE 2

Initial Laser Tube Experimental Results

<u>Experiment Number</u>	<u>NO cm Hg</u>	<u>Ar cm Hg</u>	<u>%NO/%Ar</u>	<u>O<sub>3</sub> Generated at 100V 0.020 SCPM</u>	<u>Lasing</u>
1	18.5	55.5	25/75	undetermined	undetermined
2	37.0	37.0	50/50	undetermined	undetermined
3	55.5	18.5	75/50	undetermined	undetermined
4	62.9	11.1	85/15	undetermined	undetermined
5	70.3	3.7	95/5	undetermined	undetermined
6	24.0	0	100/0	undetermined	undetermined
7	60.0	0	100/0	undetermined	undetermined



### C. Modified Laser Tube

1. Modified Laser Tube-Requirements--The initial laser experiments and kinetic calculations demonstrated that the time which the excited product  $\text{NO}_2$  spends in the laser cavity was too long. This allowed deactivation of the excited  $\text{NO}_2^*$  to ground state  $\text{NO}_2$  through collisions with other species present in the system and the wall. One of the requirements of lasing was population inversion and ground state  $\text{NO}_2$  produced by deactivation steps would prevent lasing. The volume flow rates were tabulated as a function of pressures between 0.523 torr to 1.96 torr (see Table 3). This range of pressure covered the range in which argon/ $\text{O}_3$  flowmeter operates.

Table 3 shows the velocities calculated from experimentally measured volume flows and the cross-sectional area of the flow tube. A Matheson 601 Flowmeter with stainless steel float was calibrated and used to measure the flow capacity of the pump. The cross-sectional area of the laser tube was  $3.732 \text{ cm}^2$ . The velocity in cm/sec was calculated from

$$\text{Velocity} = \frac{\text{gas volume flow}}{\text{sec}} \times \frac{760}{P_{\text{torr}}} \times \frac{1}{\text{cross-sectional area of tube}}$$

The time for the gas to reach the outlet tubing was calculated from this velocity by using the length of the initial

TABLE 3

Velocity Calculations Flowmeter--Matheson #601 (Gas Used--O<sub>2</sub>)

<u>Readings</u>		<u>ATP</u>	<u>ATP</u>	<u>Residence Time</u>		
<u>Stainless Steel Ball</u>	<u>Black Glass Ball</u>	<u>Pressure (torr)</u>	<u>Flow Rate cm<sup>3</sup>/sec</u>	<u>Velocity cm/sec</u>	<u>Initial Laser Tube (L = 24.19 cm) time (sec)</u>	<u>Modified Laser Tube (L = 2.68 cm) time (sec)</u>
50	107	0.131	0.93	1445.4	16.7x10 <sup>-3</sup>	1.26x10 <sup>-3</sup>
60	120	0.327	1.13	703.6	34.4x10 <sup>-3</sup>	2.59x10 <sup>-3</sup>
70	139	0.523	1.35	525.6	46.0x10 <sup>-3</sup>	3.47x10 <sup>-3</sup>
80	over	0.719	1.60	453.1	53.4x10 <sup>-3</sup>	4.0x10 <sup>-3</sup>
90	over	0.915	1.90	422.8	57.2x10 <sup>-3</sup>	4.3x10 <sup>-3</sup>
105	over	1.176	2.40	415.5	58.2x10 <sup>-3</sup>	4.38x10 <sup>-3</sup>
114	over	1.438	2.75	389.4	62.0x10 <sup>-3</sup>	4.68x10 <sup>-3</sup>
120	over	1.503	2.95	399.6	60.5x10 <sup>-3</sup>	4.56x10 <sup>-3</sup>
130	over	1.764	3.35	386.7	62.6x10 <sup>-3</sup>	4.72x10 <sup>-3</sup>
140	over	1.830	3.90	433.9	55.8x10 <sup>-3</sup>	4.20x10 <sup>-3</sup>
150	over	1.960	4.35	451.9	53.5x10 <sup>-3</sup>	4.0x10 <sup>-3</sup>

$$\text{Velocity (cm/sec)} = \frac{\text{gas volume flow (cm}^3\text{)}}{\text{sec}} \times \frac{760}{P \text{ (torr)}} \times \frac{1}{\text{cross-sectional area (cm}^2\text{)}}$$

$$\text{Residence time (sec)} = L \times \frac{1}{\text{velocity}}$$

laser tube (L) at various velocity:

$$\text{Time (sec)} = L \times \frac{1}{\text{velocity}}$$

These were all calculated in the assumption that L is 24.19 cm. The residence time of reactions in the tube should be long enough for production, via reaction of optimal population inversion, but less than the time where deactivation of the  $\text{NO}_2^{\neq}$  eliminates the population inversion.

2. Modified Laser Tube-Construction--The modified laser tube was made from Pyrex, internal diameter of 2.63 cm. The inlet for the reactants and outlet for the products constructed in the sides of the tube as shown in Figure 7. The inlet tubing has an outside diameter of 1.2 cm and the outlet tubing internal diameter was 1.8 cm. A second smaller tube with an internal diameter of 0.35 cm was attached to the inlet tubing at an angle of  $50^\circ$ . This small tubing served as the inlet for the NO gas. The NO gas inlet was 1.27 cm away from the laser tube itself and still was part of the main inlet. A small Tygon tubing internal extension was inserted into this inlet so as to inject the NO directly into laser cavity so the reaction would initiate just at the beginning of the cavity. The exhaust gases go directly into the vacuum pump.

The windows of the modified laser tube were two identical NaCl discs with diameters of 3.0 cm and 0.5 cm

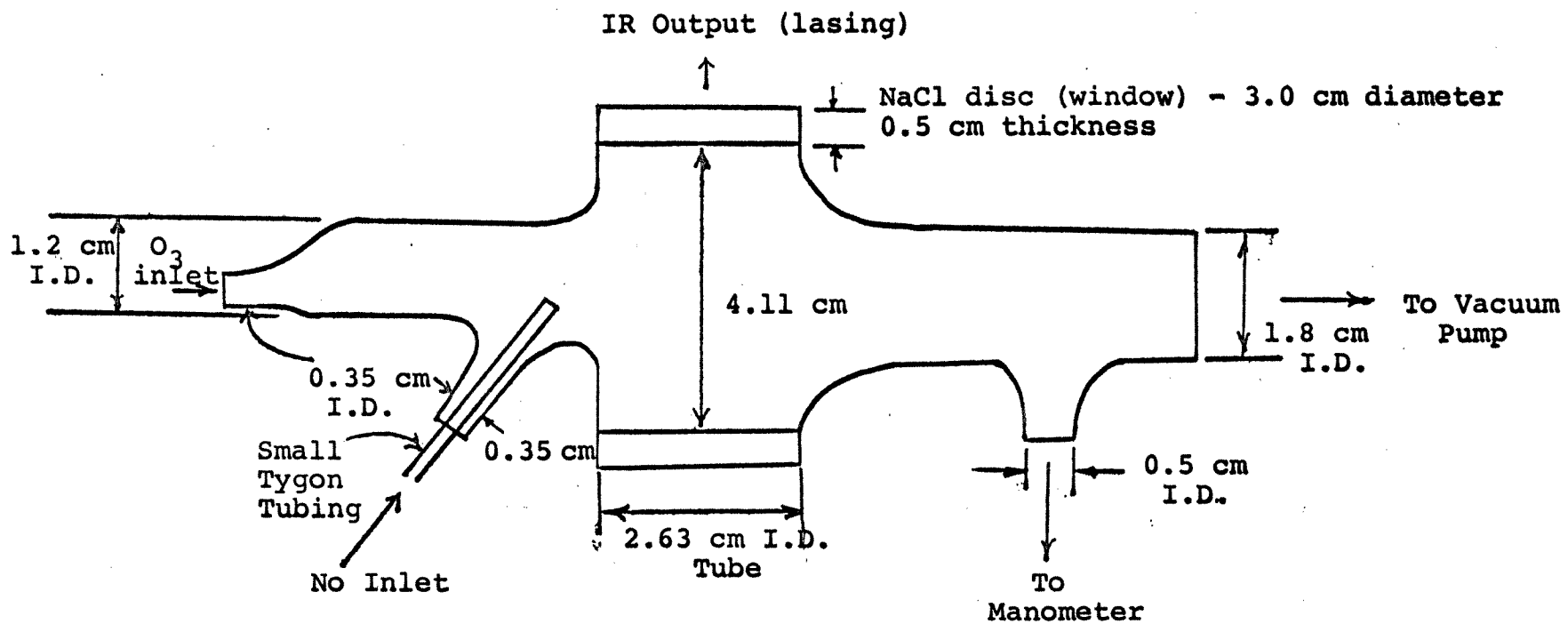


Fig. 7 Modified Laser Tube

thickness.<sup>[23]</sup> These were mounted at the two ends of the laser tube using silicon adhesive, perpendicular and not at Brewster angle. In the modified laser tube, the length for the gas to traversed was 2.68 cm and the outlet was 1.8 cm inside diameter. The cross-sectional area was  $2.54 \text{ cm}^2$ . At flow rate of  $0.93 \text{ cm}^3/\text{sec}$ , the calculated residence time was  $1.26 \times 10^{-3} \text{ sec}$ , while at initial laser tube at the same flow rate the residence time as calculated was  $16.7 \times 10^{-3} \text{ sec}$ . The modified laser tube was 13.3 times shorter in residence time at this particular flow rate than the initial laser tube. At different flow rates, the modified laser tube was close to 13.3 time shorter also, see Table 3. The shorter time is advantageous since population inversion is attained during all these times inside the tube and then deactivation will follow, but it will not hinder lasing since it will be occurring at the time the deactivated species is in the outlet through the pump.

3. Cavity--The mirrors used for the resonant cavity of the modified laser tube were exactly the same as the one used in the initial laser tube. The main difference being the distance between the two mirrors. In the initial laser cavity, the two mirrors were 42.4 cm apart, while in this modified laser cavity, the distance was only 7.47 cm. Everything else was identical, the dimensions, one flat and one concave, the aperture opening in the concave mirror

and the percent reflectance.

The stability condition,  $0 < g_1 g_2 < 1$ , which was defined earlier in section A-2, was shown in this modified laser tube to still have stability,  $g_1 g_2 = 0.9751$ , although it was a little less stable compared to  $g_1 g_2$  of the initial laser tube which was 0.8587. The intercavity distance  $L$ , was one variability which could be experimented with to obtain the optimum distance required to effect ideal resonation. As shown before,  $g_1 g_2$  could be between 0 and 1, this means that 0.5 is the ideal value for the stability condition. Therefore the equation  $g_1 = 1 - \frac{L}{r_1}$  and  $g_2 = 1 - \frac{L}{r_2}$

where  $r_1 = 300$  cm (radius for the concave mirror)

$r_2 = \infty$  (for the flat mirror)

and

$$g_1 g_2 = 0.5$$

would be equated after substitution of the values of  $r_1$  and  $r_2$  as:

$$g_1 g_2 = \left(1 - \frac{L}{r_1}\right) \times \left(1 - \frac{L}{r_2}\right)$$

$$0.5 = \left(1 - \frac{L}{300}\right) \times \left(1 - \frac{L}{\infty}\right)$$

if we neglect  $\frac{L}{\infty}$ , we have  $0.5 = 1 - \frac{L}{300}$ , and solving for  $L$ , we obtained  $L = 150$  cm as the most ideal length of the resonant cavity with the given radius of  $r_1$  and  $r_2$ .

#### 4. Reference Light, Chopper and Reference Light

Detector--The reference light, chopper and solar cell used for the modified laser tube were identical to those of the initial laser tube. The only difference was in the positioning as required by the change in the size of the laser tube. The chopper was moved as close as possible to the laser mirror and the reference light and reference light detector followed also by coming closer to the chopper.

5. Nitric Oxide--The nitric oxide gas used in the modified laser tube contained in a cylinder at the same percentage of purity as previously reported.

Several changes were instituted in the nitric oxide flow system with this modified laser tube. Argon gas was not premixed with NO, but, instead, pure NO gas was fed into the laser tube to react with the ozone. Another change was the installment of a calibrated flowmeter between the cylinder and the needle valve to monitor the rate of NO gas flowing in the system.

6. Calibration of NO and Ar/O<sub>3</sub> Flowmeters--The NO flowmeter was a Brooks Instrument Division, tube size R-2-15-AAA. A small black glass ball served as a float indicating the flow in readings which ranged from 0 to 15 and corresponded to NO flows at 0 to 0.95 cm<sup>3</sup>/sec at ATP.

Nitrogen gas was used to calibrate this flowmeter, a 10 ml soap bubble flowmeter and a timer accurate to 0.1

second. As nitrogen gas flow was varied from the cylinder into the flowmeter, the float indicated the heading. The outlet gas was input to the bubble flowmeter inlet. A bubble was generated in the tube ahead of the gas stream which was carried upward by the flowing nitrogen gas. The time for this bubble to flow over a known volume, say 5 or 10 ml in seconds, yielded the flow rate in ml per second. Varying the nitrogen flow gave a series of flow rates versus the float heading. This was tabulated in Table 4 and the graph is shown in Figure 8. Since we were interested in the NO gas and not the nitrogen, we converted the flow rates of nitrogen into NO using the formula

$$\frac{R_{NO}}{R_{N_2}} = \sqrt{\frac{m_{N_2}}{m_{NO}}} = 0.966$$

where  $R_{NO}$  = velocity of the gas, NO

$R_{N_2}$  = velocity of the gas,  $N_2$

$m_{N_2}$  = mass of the nitrogen gas

$m_{NO}$  = mass of the NO gas

The data for NO gas are shown in Table 5, the corresponding graph versus the flow reading is shown in Figure 8.

The Ar/O<sub>3</sub> flowmeter used was a Matheson #601 with an internal diameter of 0.28 mm and a scale from 0 to 150. Two floats were used, one a black glass ball and the other a stainless steel ball. The black glass ball was lighter



TABLE 4NO Flowmeter Calibration

Brooks Instrument Division, Hatfield, PA

Tube Size R-2-15-AAA

Black Glass Float - Reading bottom of the ball

Gas - nitrogen

<u>Volume, cm<sup>3</sup></u> <u>Atm pressure</u> <u>room temp</u>	<u>Time, sec</u>	<u>Gas Volume Flow</u> <u>cm<sup>3</sup>/sec</u>	<u>Flowmeter</u> <u>Reading</u>
10	103.4	0.097	1.9
5	30.8	0.16	3.7
10	33.9	0.29	6.4
10	25.9	0.39	7.9
10	21.0	0.48	9.2
10	19.0	0.53	9.9
10	16.9	0.59	10.7
10	15.5	0.65	11.4
10	12.8	0.78	13.1
10	10.8	0.93	14.7

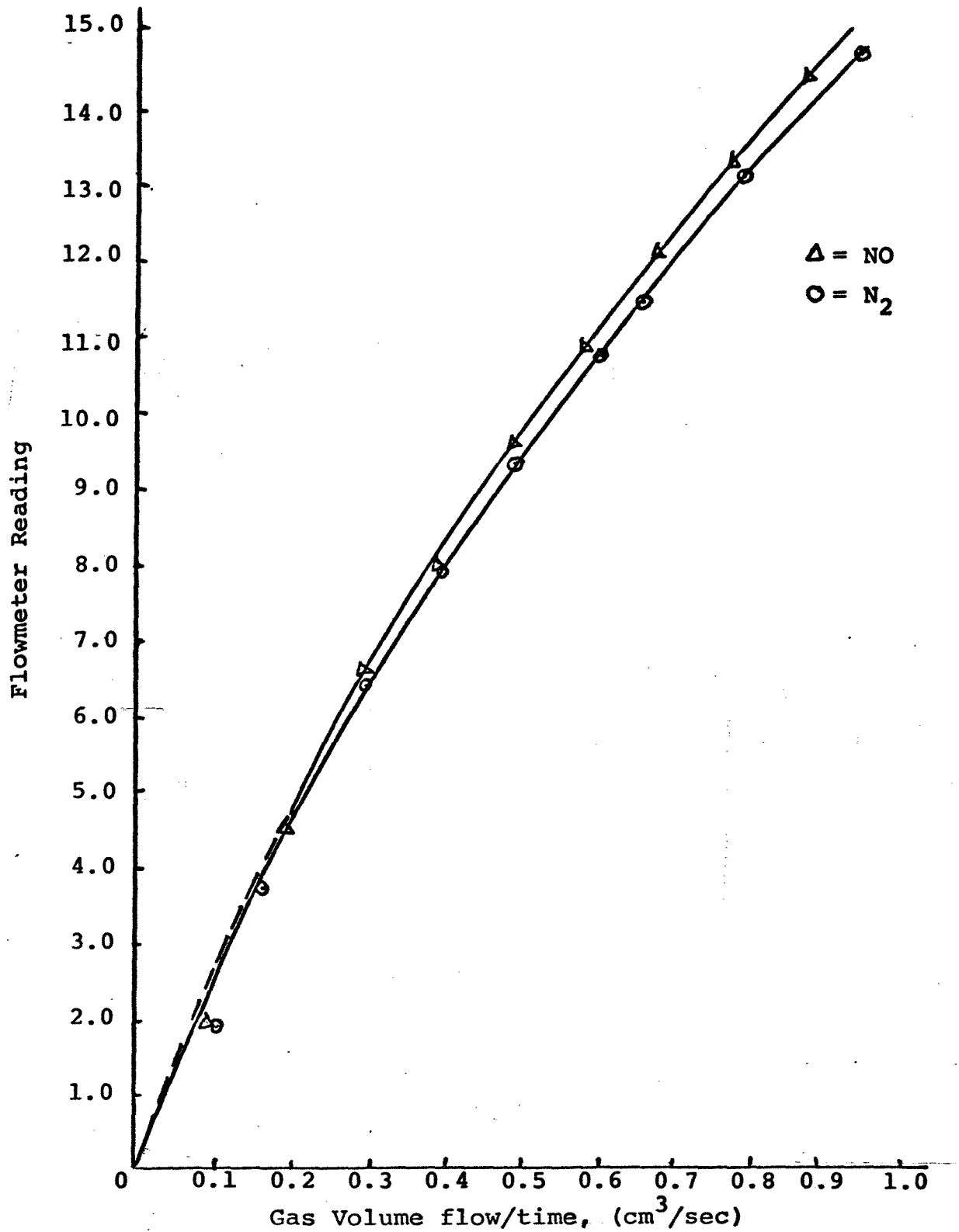


Fig. 8 NO Flowmeter Calibration

TABLE 5

$$\frac{R_{NO}}{R_{N_2}} = \frac{\overline{M_{N_2}}}{M_{NO}} = \sqrt{\frac{28}{30}}$$

$$R_{NO} = 0.966 R_{N_2}$$

Flow rate, cm <sup>3</sup> /sec Nitrogen, $R_{N_2}$	Flow rate, cm <sup>3</sup> /sec NO, $R_{NO}$
0.1	0.0966
0.2	0.1932
0.3	0.2898
0.4	0.3864
0.5	0.4830
0.6	0.5796
0.7	0.6762
0.8	0.7728
0.9	0.8694
1.0	0.966

and indicated flows corresponding from 0 to less than 1.5 cm<sup>3</sup>/sec, where as the stainless steel ball covered the flows from 0 to about 4.0 cm<sup>3</sup>/sec.

The calibration of this flowmeter was exactly the same as the NO flowmeter calibration, except the gas used was argon. Varying the argon flow over the entire range of the flowmeter gave a series of flow rates versus the readings in both the stainless steel ball and the black glass ball. These were tabulated in Table 6 and the graphs are shown in Figures 9 and 10.

TABLE 6

Ar/O<sub>3</sub> Flowmeter Calibration

Matheson #601 Bottom of Ball

<u>Stainless Steel Ball</u>	<u>Black Ball</u>	<u>Volume cm<sup>3</sup></u>	<u>Time, sec</u>	<u>Argon Vol/Time, cm<sup>3</sup>/sec</u>
48	105	10	13.8	0.72
0	25	3	26.9	0.11
40	93	10	15.9	0.63
63	126	10	9.7	1.03
6	41	10	43.5	0.23
14	50	10	35.6	0.28
28	72	10	22.3	0.45
67	137	10	8.6	1.16
65	132	10	9.0	1.11
78	over	10	7.2	1.39
93	over	10	5.7	1.75
110	over	10	4.3	2.33
129	over	10	3.3	3.03
141	over	10	2.8	3.6
149	over	10	2.7	3.7

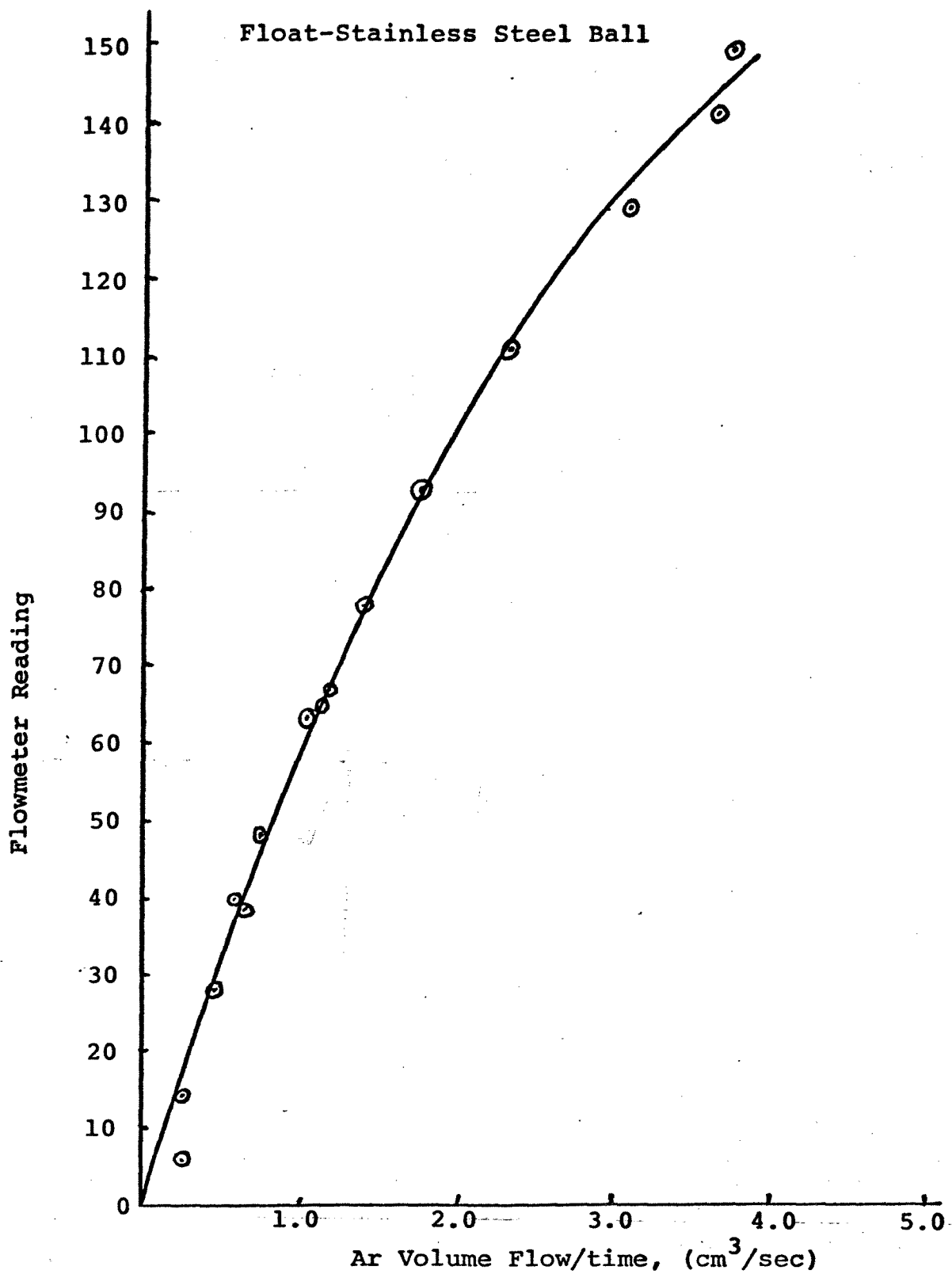


Fig. 9 Ar/O<sub>2</sub> Flowmeter Calibration

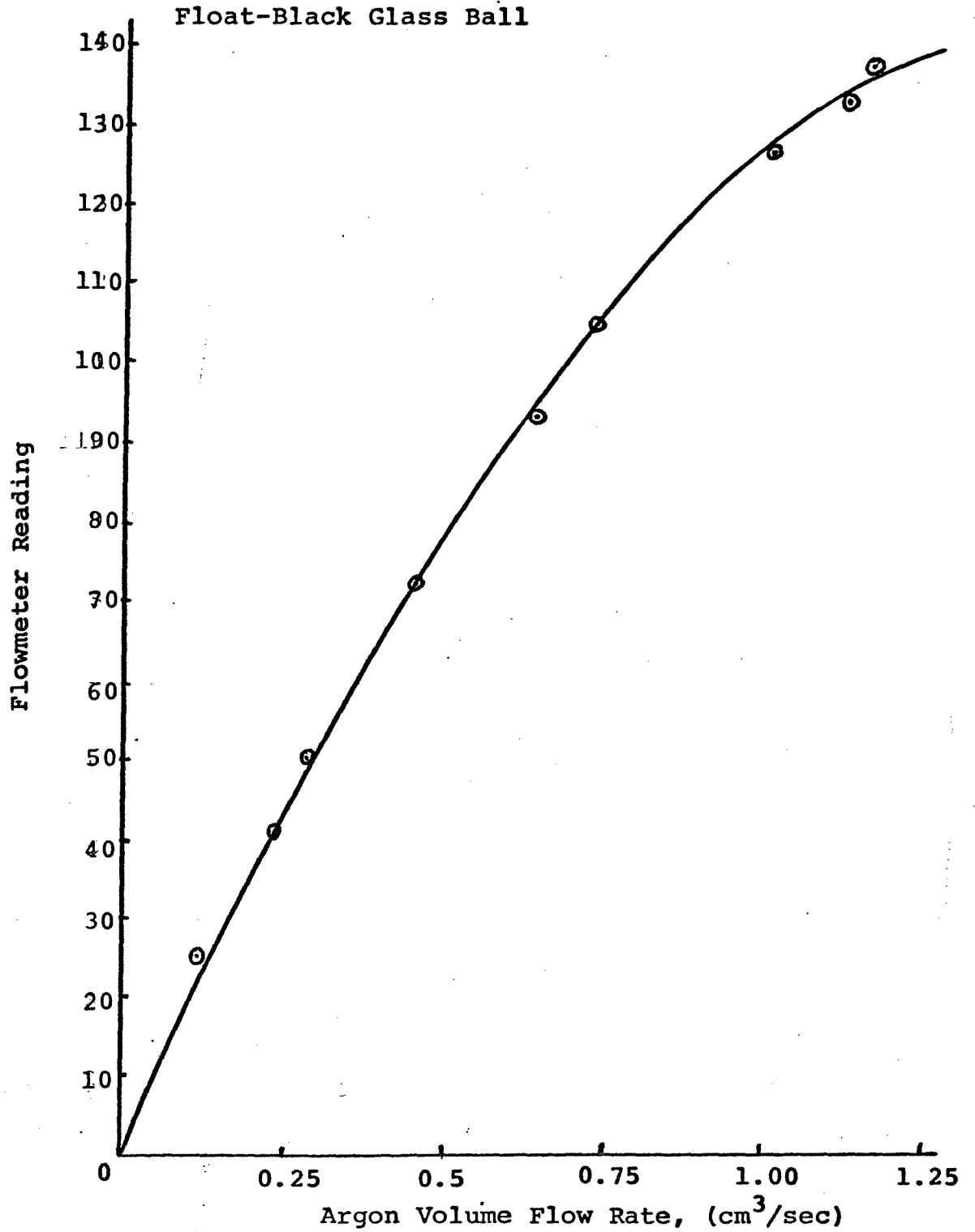


Fig. 10 Ar/O<sub>3</sub> Flowmeter Calibration

#### D. Experiments Using the Modified Laser Tube

The modified laser tube and cavity experiments were conducted in a very similar manner as the initial laser experiments, except for the following changes which were discussed previously:

1. The modified laser tube was much shorter than the initial laser tube (Section II-C2). Thus, residence time of reaction was in the range of 1.26 to 4.72 milliseconds.
2. The resonant cavity was shorter (Section II-C3) affecting the gain equation as discussed in Section IV.
3. NO and Ar/O<sub>3</sub> flowmeters were used to monitor the flows.

The variables, constants and results were tabulated in Table 7. Unfortunately, the results, as indicated, were undetermined whether there was lasing or not. For further discussion see Section Results and Discussion.



TABLE 7  
Modified Laser Tube Experimental Results

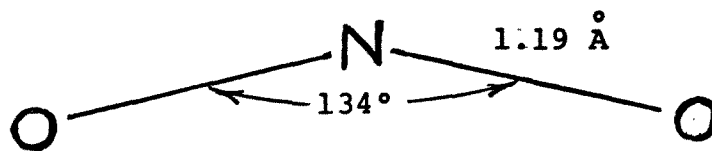
<u>Total Pressure</u>		<u>NO Flow Rate</u>		<u>Ar/O<sub>3</sub> Flow Rate</u>		<u>Total Flow</u>	<u>Lasing</u>
<u>cm of oil</u>	<u>mm Hg</u>	<u>Reading</u>	<u>cm<sup>3</sup>/sec</u>	<u>Reading</u>	<u>cm<sup>3</sup>/sec</u>	<u>NO + Ar/O<sub>3</sub> cm<sup>3</sup>/sec</u>	<u>Yes/No/Undetermined</u>
0.9-1.1	0.65	1	0.045	5	0.15	0.195	Undetermined
0.9-1.1	0.65	2	0.1	5	0.15	0.25	Undetermined
0.9-1.1	0.65	5	0.21	5	0.15	0.36	Undetermined
0.9-1.1	0.65	1	0.045	15	0.275	0.32	Undetermined
0.9-1.1	0.65	2	0.1	15	0.275	0.375	Undetermined
0.9-1.1	0.65	1	0.045	30	0.275	0.32	Undetermined
0.9-1.1	0.65	5	0.21	30	0.48	0.69	Undetermined
0.9-1.1	0.65	1	0.045	5	0.15	0.195	Undetermined
0.9-1.1	0.65	1	0.045	10	0.23	0.275	Undetermined
0.9-1.1	0.65	1	0.045	15	0.275	0.32	Undetermined
0.9-1.1	0.65	1	0.045	30	0.275	0.32	Undetermined
0.9-1.1	0.65	2	0.1	5	0.15	0.25	Undetermined
0.9-1.1	0.65	2	0.1	15	0.275	0.375	Undetermined
0.9-1.1	0.65	5	0.21	5	0.15	0.36	Undetermined
8.0	5.2	10	0.515	140	3.45	3.965	Undetermined
8.0	>5.2	>15	>0.93	150	>3.875	>4.8	Undetermined

### III. THEORY

#### A. The NO<sub>2</sub> Molecule

The NO<sub>2</sub> molecule has a bent geometry, see Fig. 11. The nitrogen atom is located between two oxygen atoms and makes an angle of 134°. [24] The N-O distance is 1.19 Å.

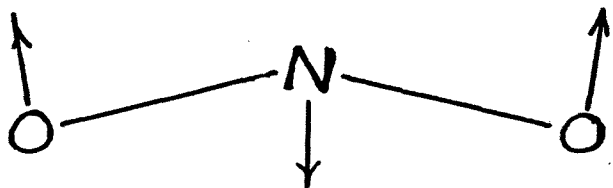
The three fundamental modes of vibrations of the NO<sub>2</sub> molecule are symmetric stretching ( $\nu_1$ ), bending mode ( $\nu_2$ ) and the antisymmetric stretching ( $\nu_3$ ). [25] The diagram of these modes of vibration is seen in Fig. 12.  $\nu_1$ ,  $\nu_2$  and  $\nu_3$  were found to have the values in wave numbers of 1320 cm<sup>-1</sup> (7.57 μm), 648 cm<sup>-1</sup> (15.43 μm) and 1621 cm<sup>-1</sup> (6.2 μm). [25] In terms of energies,  $\nu_1$ ,  $\nu_2$  and  $\nu_3$  correspond to  $2.62 \times 10^{-13}$ ,  $1.28 \times 10^{-13}$  and  $3.21 \times 10^{-13}$  ergs. The energy level diagram of the three fundamental modes of vibrations is shown in Fig. 13. [26] Transitions from one energy level into another energy level is equivalent to the difference between the two energy levels,  $\Delta E = E_2 - E_1 = h\nu$ .

Fig. 11 The NO<sub>2</sub> Molecule

Symmetric Stretching  
( $\nu_1$ )

$$\bar{\nu}_1 = 1320 \text{ cm}^{-1}$$

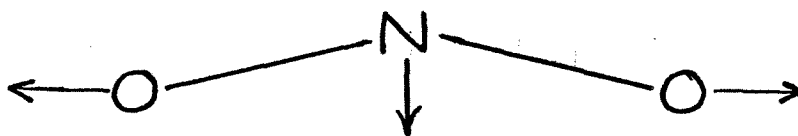
$$\lambda_1 = 7.57 \text{ } \mu\text{m}$$



Bending Mode ( $\nu_2$ )

$$\bar{\nu}_2 = 648 \text{ cm}^{-1}$$

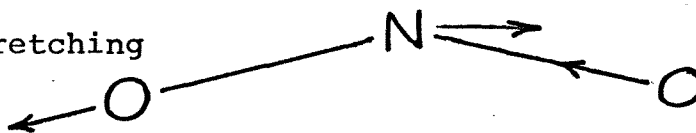
$$\nu_2 = 15.43 \text{ } \mu\text{m}$$



Antisymmetric Stretching  
( $\nu_3$ )

$$\bar{\nu}_3 = 1611 \text{ cm}^{-1}$$

$$\lambda_3 = 6.2 \text{ } \mu\text{m}$$

Fig. 12 Fundamental Modes of Vibrations of NO<sub>2</sub> Molecule

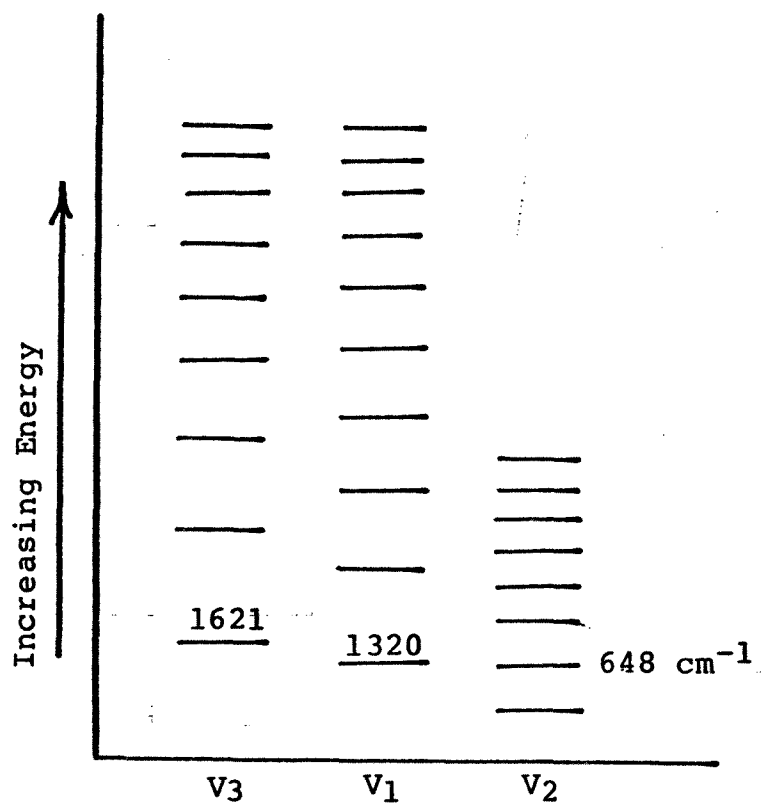
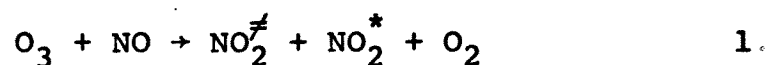


Fig. 13 Fundamental Vibrations of NO<sub>2</sub> with Associated Energy Level Spacings

## B. Reactions

The gas phase reaction of  $O_3$  and  $NO$  at low pressures (below 10 torr) produces vibrational and electronically excited products,  $NO_2^{\neq}$  and  $NO_2^*$  according to the equation:



At room temperature the reaction proceeds with approximately 93% vibrationally excited  $NO_2^{\neq}$  and 7% electronically excited  $NO_2^*$ . [18] This reaction has been studied earlier by several investigators, namely: Clough and Thrush, [15] Stair and Kennealy. [27] More recent workers include Golde and Kaufman, [18] Hampson, et al.; [28] and Birks. et al. [29]

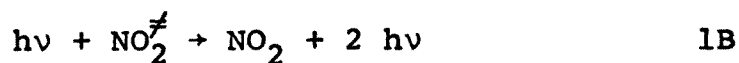
The vibrationally excited  $NO_2^{\neq}$  through spontaneous emission gives off photons ( $h\nu$ ) as seen by this equation:



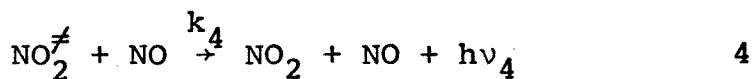
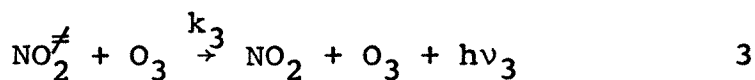
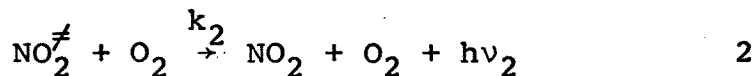
The photons ( $h\nu$ ) have been observed centering in the IR at 1.5  $\mu m$  and 3.6  $\mu m$  wavelengths by Golde and Kaufman. [18] The 1.5  $\mu m$  and 3.6  $\mu m$  wavelengths from one molecule of  $NO_2^{\neq}$  formed in the reaction of  $O_3$  and  $NO$ , correspond by calculation to 19 kcal/mole and 7.9 kcal/mole.

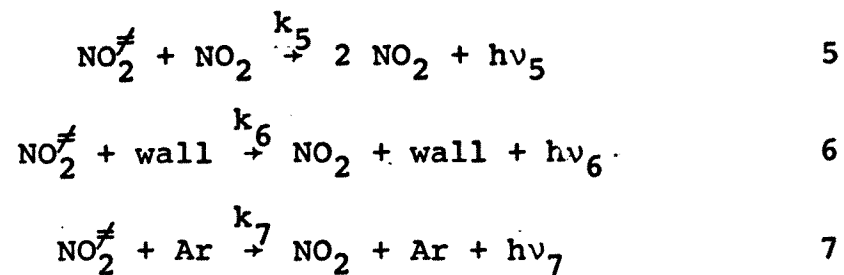
It is hoped in this work that the photons,  $h\nu$ , with the given wavelengths centering in 1.5  $\mu m$  and 3.6  $\mu m$  can

be utilized to effect stimulated emissions by



Equation 1B shows that the amount of energy  $h\nu$  is doubled, i.e. amplified, and this is the basis for lasing. There are three basic requirements for lasing and they are (a) an active medium which, in this case, is  $\text{NO}_2^{\neq}$ ; (b) population inversion, that is the  $\text{NO}_2^{\neq}$  species greater than the ground state  $\text{NO}_2$ ; and (c) a resonant cavity, which was fully discussed previously in Section II. (a) and (c) can easily be obtained, but (b), the population inversion, is difficult to have. In this study, the system operates in such a way that deactivation of the excited species  $\text{NO}_2^{\neq}$  by other gas phase species and the vessel wall is significant. Some of these species are the ground state  $\text{NO}_2$ , the  $\text{O}_2$  formed in the product, the unreacted  $\text{NO}$ ,  $\text{O}_3$  and the carrier argon, in addition to collisions with the wall of the reaction vessel. The deactivation processes occur during the same time the vibrationally excited  $\text{NO}_2$  species are formed due to the relative slowness of the  $\text{O}_3 + \text{NO}_2$  reaction.

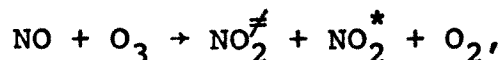




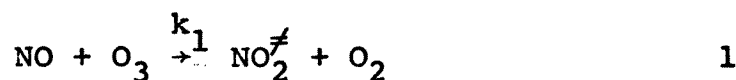
These equations, 1 to 7, are the heart of the computer programming as discussed in the following section, Kinetics, III-C.

### C. Kinetics

The primary reaction



assuming negligible amounts of electronically excited  $\text{NO}_2^*$ , is written as



The reaction rate of this equation will be

$$\frac{d[\text{NO}_2^\ddagger]}{dt} = k_1 [\text{NO}] [\text{O}_3],$$

however, the vibrationally excited  $\text{NO}_2^\ddagger$  produced by the above reaction collided with the other species present in the reactor tube and lose its vibrational energy via translational energy transfer to these other species. It therefore becomes deactivated to its ground level, this is shown in equations 2, 3, 4, 5, 6 and 7. Within a certain length of time, this relaxation of the  $\text{NO}_2^\ddagger$  creates more  $\text{NO}_2^0$  than the excited species and lasing can not occur, due to lack of population inversion. Incorporation of these losses into the reaction equation gives:

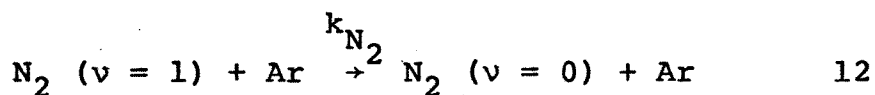
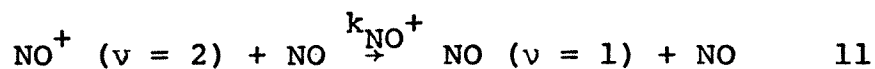
$$\begin{aligned} \frac{d[\text{NO}_2^\ddagger]}{dt} = & k_1 [\text{NO}] [\text{O}_3] - \{ k_2 [\text{NO}_2^\ddagger] [\text{O}_2] + k_3 [\text{NO}_2^\ddagger] [\text{O}_3] + \\ & k_4 [\text{NO}_2^\ddagger] [\text{NO}] + k_5 [\text{NO}_2^\ddagger] [\text{NO}_2] + k_6 [\text{NO}_2^\ddagger] [\text{wall}] + \\ & k_7 [\text{NO}_2^\ddagger] [\text{Ar}] \} \end{aligned} \quad 9$$



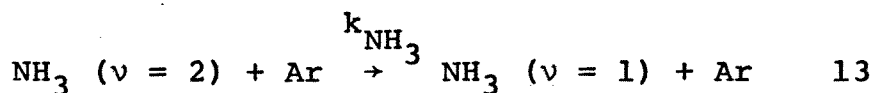
Solution to equation 9 gives the amount of excited  $\text{NO}_2^{\ddagger}$  at any particular instant in time of the reaction for the given initial concentrations. It also considers the losses due to collisions with the other species. A computer program was designed to solve this reaction rate equation and it is listed in the Appendix. The first rate constant,  $k_1$ , was found to be

$$k_1 = 9 \times 10^{-13} e^{-1200/T}, \text{ cm}^3/\text{molecules} - \text{sec} \quad 10$$

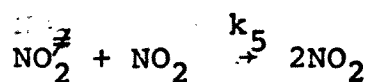
within the temperature range  $198^\circ\text{K}$  to  $330^\circ\text{K}$ . [28] At  $20^\circ\text{C}$ ,  $k_1$  is equal to  $1.61 \times 10^{-14} \text{ cm}^3/\text{molecules} - \text{sec}$ . For equations 2, 3 and 4, the rate constants were  $5.1 \times 10^{-13}$ ,  $2.57 \times 10^{-13}$  and  $1.8 \times 10^{-12} \text{ cm}^3/\text{molecules} - \text{sec}$ , respectively and were found in the study by Kin-Kwok Hui and T.A. Cool. [20] There were no available rate constants in the literature for equations 5 and 7. An extensive search for vibrational relaxation of other species which very closely resemble equations 5 and 7 yielded the following equations for consideration.



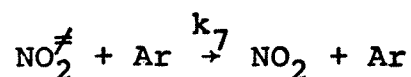
and



Equation 11 was assumed to be similar to equation 5:



and therefore  $k_{\text{NO}^{\ddagger}}$  was adapted as  $k_5$  which is equal to  $3.0 \times 10^{-13} \text{ cm}^3/\text{molecule} \cdot \text{sec.}$  [30] The rate constant of equation 6 was  $250 \text{ cm}^3/\text{molecule} \cdot \text{sec.}$  [18] Whereas equations 12 and 13 were taken as similar to equation 7:



and both values of the rate constants which were  $1.8 \times 10^{-18}$  (equation 12) and  $1.8 \times 10^{-13}$  (equation 13) were run separately in the programming plus a value intermediate of the two,  $1.8 \times 10^{-15} \text{ cm}^3/\text{molecules} \cdot \text{sec.}$  Equations 12 and 13 were taken from reference [31] and [32].

The NO concentration was varied and  $\text{O}_3$  was held constant. Five values of NO concentration were fed into the programs for each value of  $k_7$ , these were  $5.0 \times 10^{11}$ ,  $5.0 \times 10^{12}$ ,  $5.0 \times 10^{13}$ ,  $5.0 \times 10^{14}$  and  $5.0 \times 10^{15} \text{ molecules/cm}^3$  where  $\text{O}_3$  remained as  $2.0 \times 10^{11} \text{ molecules/cm}^3$ . Runs 1 to 5 were run with  $k_7$  as  $1.8 \times 10^{-13}$ , runs 6 to 10 adopted the intermediate value of  $1.8 \times 10^{-15}$  and runs 11 to 15,  $k_7$  as  $1.8 \times 10^{-18} \text{ cm}^3/\text{molecule} \cdot \text{sec.}$  Tables 8, 9 and 10 showed the results obtained in the print out of the program.

Run #6 was a typical run showing the formation of the excited species  $\text{NO}_2^{\ddagger}$  and the ground state species  $\text{NO}_2^{\circ}$  with

time from the start of the reaction, see Figure 11. It also showed the time ( $t_{\max}$ ) when the population inversion was at a maximum  $(NO_2^{\#})_{\max}$ . Figure 12 was taken from the observation of Runs #6 to #10. The effect of increasing amounts of NO concentration was plotted against the time of maximum population inversion,  $t_{\max}$ . It showed that  $t_{\max}$  had larger values (longer) at lower amounts of NO concentration with the given constant  $O_3$  concentration. Figure 13 was taken also from Run #6 to Run #10. It showed the effect of increasing the NO concentration in the formation of maximum population of the excited  $NO_2^{\#}$ . The graph clearly indicated an increasing tendency of  $NO_2^{\#}(\max)$  with increasing NO concentration. For further discussion of results see Section IV, Results and Discussion.

The following observations were used in the programming:

k1 to k7 - the rate constants of the equation 1 to 7  
 $cm^3/molecule - sec$

$O_3$  - ozone concentration, molecules/ $cm^3$

NO - nitric oxide concentration, molecules/ $cm^3$

AR - argon concentration, molecules/ $cm^3$

DELTA - time interval where observation was made, sec

T - time, sec

$NO_2M$  - vibrationally excited  $NO_2^{\#}$  made, regardless of losses due to collisions, molecules/ $cm^3$

$NO_2L$  - vibrationally excited  $NO_2^{\#}$  lost due to collisions

with other species and wall, molecules/cm<sup>3</sup>

NO2E - net amount of vibrationally excited NO<sub>2</sub><sup>\*</sup> after losses were considered, molecules/cm<sup>3</sup>

NO2G = NO2 - ground level NO<sub>2</sub> as a result of collisions with the other species and the wall, molecules/cm<sup>3</sup>

There were five concentrations of NO,  $5 \times 10^{11}$ ,  $5 \times 10^{12}$ ,  $5 \times 10^{13}$ ,  $5 \times 10^{14}$  and  $5 \times 10^{15}$  molecules/cm<sup>3</sup>. These were available as data cards in the programming.

TABLE 8

Summary of Programming Results--Run No. 1 to Run No. 5

Observations Constants & Variables	Run No.				
	<u>1</u>	<u>2</u>	<u>3</u>	<u>4</u>	<u>5</u>
NO ( $\frac{\text{molecules}}{\text{cm}^3}$ )	$5.0 \times 10^{11}$	$5.0 \times 10^{12}$	$5.0 \times 10^{13}$	$5.0 \times 10^{14}$	$5.0 \times 10^{15}$
O <sub>3</sub> ( $\frac{\text{molecules}}{\text{cm}^3}$ )	$2.0 \times 10^{11}$	$2.0 \times 10^{11}$	$2.0 \times 10^{11}$	$2.0 \times 10^{11}$	$2.0 \times 10^{11}$
Ar ( $\frac{\text{molecules}}{\text{cm}^3}$ )	$6.0 \times 10^{16}$	$6.0 \times 10^{16}$	$6.0 \times 10^{16}$	$6.0 \times 10^{16}$	$6.0 \times 10^{16}$
K1 ( $\frac{\text{cm}^3}{\text{molecule-sec}}$ )	$1.61 \times 10^{-14}$	$1.61 \times 10^{-14}$	$1.61 \times 10^{-14}$	$1.61 \times 10^{-14}$	$1.61 \times 10^{-14}$
K2 ( $\frac{\text{cm}^3}{\text{molecule-sec}}$ )	$5.1 \times 10^{-13}$	$5.1 \times 10^{-13}$	$5.1 \times 10^{-13}$	$5.1 \times 10^{-13}$	$5.1 \times 10^{-13}$
K3 ( $\frac{\text{cm}^3}{\text{molecule-sec}}$ )	$2.57 \times 10^{-13}$	$2.57 \times 10^{-13}$	$2.57 \times 10^{-13}$	$2.57 \times 10^{-13}$	$2.57 \times 10^{-13}$
K4 ( $\frac{\text{cm}^3}{\text{molecule-sec}}$ )	$1.8 \times 10^{-12}$	$1.8 \times 10^{-12}$	$1.8 \times 10^{-12}$	$1.8 \times 10^{-12}$	$1.8 \times 10^{-12}$
K5 ( $\frac{\text{cm}^3}{\text{molecule-sec}}$ )	$3.0 \times 10^{-13}$	$3.0 \times 10^{-13}$	$3.0 \times 10^{-13}$	$3.0 \times 10^{-13}$	$3.0 \times 10^{-13}$
K6 ( $\frac{\text{cm}^3}{\text{molecule-sec}}$ )	250	250	250	250	250
K7 ( $\frac{\text{cm}^3}{\text{molecule-sec}}$ )	$1.8 \times 10^{-13}$	$1.8 \times 10^{-13}$	$1.8 \times 10^{-13}$	$1.8 \times 10^{-13}$	$1.8 \times 10^{-13}$
NO <sub>2</sub> <sup>‡</sup> (max) ( $\frac{\text{molecule}}{\text{cm}^3}$ )	$8.05 \times 10^4$	$8.05 \times 10^5$	$8.05 \times 10^6$	$8.05 \times 10^4$	$8.05 \times 10^8$
Time @ NO <sub>2</sub> <sup>‡</sup> (max) (sec)	$5.0 \times 10^{-5}$	$5.0 \times 10^{-5}$	$5.0 \times 10^{-5}$	$5.0 \times 10^{-5}$	$5.0 \times 10^{-5}$
NO <sub>2</sub> <sup>‡</sup> = NO <sub>2</sub> ( $\frac{\text{molecules}}{\text{cm}^3}$ )	$1.3 \times 10^5$	$1.3 \times 10^6$	$1.3 \times 10^7$	$1.3 \times 10^8$	$8.0 \times 10^8$
Time NO <sub>2</sub> <sup>‡</sup> = NO <sub>2</sub> (sec)	$1.75 \times 10^{-4}$	$1.75 \times 10^{-4}$	$1.75 \times 10^{-4}$	$1.75 \times 10^{-4}$	$1.0 \times 10^{-4}$

TABLE 9  
Summary of Programming Results--Run No. 6 to 10

Observations Constants & Variables	Run No.				
	<u>6</u>	<u>7</u>	<u>8</u>	<u>9</u>	<u>10</u>
NO ( $\frac{\text{molecules}}{\text{cm}^3}$ )	$5.0 \times 10^{11}$	$5.0 \times 10^{12}$	$5.0 \times 10^{13}$	$5.0 \times 10^{14}$	$5.0 \times 10^{15}$
O <sub>3</sub> ( $\frac{\text{molecules}}{\text{cm}^3}$ )	$2.0 \times 10^{11}$	$2.0 \times 10^{11}$	$2.0 \times 10^{11}$	$2.0 \times 10^{11}$	$2.0 \times 10^{11}$
Ar ( $\frac{\text{molecules}}{\text{cm}^3}$ )	$6.0 \times 10^{16}$	$6.0 \times 10^{16}$	$6.0 \times 10^{16}$	$6.0 \times 10^{16}$	$6.0 \times 10^{16}$
K1 ( $\frac{\text{cm}^3}{\text{molecule-sec}}$ )	$1.61 \times 10^{-14}$	$1.61 \times 10^{-14}$	$1.61 \times 10^{-14}$	$1.61 \times 10^{-14}$	$1.61 \times 10^{-14}$
K2 ( $\frac{\text{cm}^3}{\text{molecule-sec}}$ )	$5.1 \times 10^{-13}$	$5.1 \times 10^{-13}$	$5.1 \times 10^{-13}$	$5.1 \times 10^{-13}$	$5.1 \times 10^{-13}$
K3 ( $\frac{\text{cm}^3}{\text{molecule-sec}}$ )	$2.57 \times 10^{-13}$	$2.57 \times 10^{-13}$	$2.57 \times 10^{-13}$	$2.57 \times 10^{-13}$	$2.57 \times 10^{-13}$
K4 ( $\frac{\text{cm}^3}{\text{molecule-sec}}$ )	$1.8 \times 10^{-12}$	$1.8 \times 10^{-12}$	$1.8 \times 10^{-12}$	$1.8 \times 10^{-12}$	$1.8 \times 10^{-12}$
K5 ( $\frac{\text{cm}^3}{\text{molecule-sec}}$ )	$3.0 \times 10^{-13}$	$3.0 \times 10^{-13}$	$3.0 \times 10^{-13}$	$3.0 \times 10^{-13}$	$3.0 \times 10^{-13}$
K6 ( $\frac{\text{cm}^3}{\text{molecule-sec}}$ )	250	250	250	250	250
K7 ( $\frac{\text{cm}^3}{\text{molecule-sec}}$ )	$1.8 \times 10^{-15}$	$1.8 \times 10^{-15}$	$1.8 \times 10^{-15}$	$1.8 \times 10^{-15}$	$1.8 \times 10^{-15}$
NO <sub>2</sub> <sup>#</sup> (max) ( $\frac{\text{molecule}}{\text{cm}^3}$ )	$2.36 \times 10^6$	$2.3 \times 10^7$	$2.0 \times 10^8$	$7.2 \times 10^8$	$2.2 \times 10^9$
Time @ NO <sub>2</sub> <sup>#</sup> (max) (sec)	$2.0 \times 10^{-3}$	$2.0 \times 10^{-3}$	$1.8 \times 10^{-3}$	$6.0 \times 10^{-4}$	$2.0 \times 10^{-4}$
NO <sub>2</sub> <sup>#</sup> = NO <sub>2</sub> ( $\frac{\text{molecules}}{\text{cm}^3}$ )	$3.6 \times 10^6$	$3.6 \times 10^7$	$2.9 \times 10^8$	$1.0 \times 10^9$	$1.87 \times 10^9$
Time NO <sub>2</sub> <sup>#</sup> = NO <sub>2</sub> (sec)	$4.5 \times 10^{-3}$	$4.5 \times 10^{-3}$	$3.7 \times 10^{-3}$	$1.3 \times 10^{-3}$	$3.7 \times 10^{-4}$

TABLE 10

Summary of Programming Results--Run No. 11 to Run No. 15

Observations Constants & Variables	11	12	13	14	15
NO ( $\frac{\text{molecules}}{\text{cm}^3}$ )	$5.0 \times 10^{11}$	$5.0 \times 10^{12}$	$5.0 \times 10^{13}$	$5.0 \times 10^{14}$	$5.0 \times 10^{15}$
O <sub>3</sub> ( $\frac{\text{molecules}}{\text{cm}^3}$ )	$2.0 \times 10^{11}$	$2.0 \times 10^{11}$	$2.0 \times 10^{11}$	$2.0 \times 10^{11}$	$2.0 \times 10^{11}$
Ar ( $\frac{\text{molecules}}{\text{cm}^3}$ )	$6.0 \times 10^{16}$	$6.0 \times 10^{16}$	$6.0 \times 10^{16}$	$6.0 \times 10^{16}$	$6.0 \times 10^{16}$
K1 ( $\frac{\text{cm}^3}{\text{molecule-sec}}$ )	$1.61 \times 10^{-14}$	$1.61 \times 10^{-14}$	$1.61 \times 10^{-14}$	$1.61 \times 10^{-14}$	$1.61 \times 10^{-14}$
K2 ( $\frac{\text{cm}^3}{\text{molecule-sec}}$ )	$5.1 \times 10^{-13}$	$5.1 \times 10^{-13}$	$5.1 \times 10^{-13}$	$5.1 \times 10^{-13}$	$5.1 \times 10^{-13}$
K3 ( $\frac{\text{cm}^3}{\text{molecule-sec}}$ )	$2.57 \times 10^{-13}$	$2.57 \times 10^{-13}$	$2.57 \times 10^{-13}$	$2.57 \times 10^{-13}$	$2.57 \times 10^{-13}$
K4 ( $\frac{\text{cm}^3}{\text{molecule-sec}}$ )	$1.8 \times 10^{-12}$	$1.8 \times 10^{-12}$	$1.8 \times 10^{-12}$	$1.8 \times 10^{-12}$	$1.8 \times 10^{-12}$
K5 ( $\frac{\text{cm}^3}{\text{molecule-sec}}$ )	$3.0 \times 10^{-13}$	$3.0 \times 10^{-13}$	$3.0 \times 10^{-13}$	$3.0 \times 10^{-13}$	$3.0 \times 10^{-13}$
K6 ( $\frac{\text{cm}^3}{\text{molecule-sec}}$ )	250	250	250	250	250
K7 ( $\frac{\text{cm}^3}{\text{molecule-sec}}$ )	$1.8 \times 10^{-18}$	$1.8 \times 10^{-18}$	$1.8 \times 10^{-18}$	$1.8 \times 10^{-18}$	$1.8 \times 10^{-18}$
NO <sub>2</sub> <sup>≠</sup> (max) ( $\frac{\text{molecule}}{\text{cm}^3}$ )	$3.5 \times 10^6$	$3.3 \times 10^7$	$2.4 \times 10^8$	$7.3 \times 10^8$	$2.2 \times 10^9$
Time @ NO <sub>2</sub> <sup>≠</sup> (max) (sec)	$3.0 \times 10^{-3}$	$2.8 \times 10^{-3}$	$2.0 \times 10^{-3}$	$6.0 \times 10^{-4}$	$2.0 \times 10^{-4}$
NO <sub>2</sub> <sup>≠</sup> = NO <sub>2</sub> ( $\frac{\text{molecules}}{\text{cm}^3}$ )	$5.2 \times 10^8$	$5.0 \times 10^7$	$3.8 \times 10^8$	$1.1 \times 10^9$	$2.0 \times 10^9$
Time NO <sub>2</sub> <sup>≠</sup> = NO <sub>2</sub> (sec)	$6.5 \times 10^{-3}$	$6.2 \times 10^{-3}$	$4.8 \times 10^{-3}$	$1.5 \times 10^{-3}$	$3.0 \times 10^{-4}$

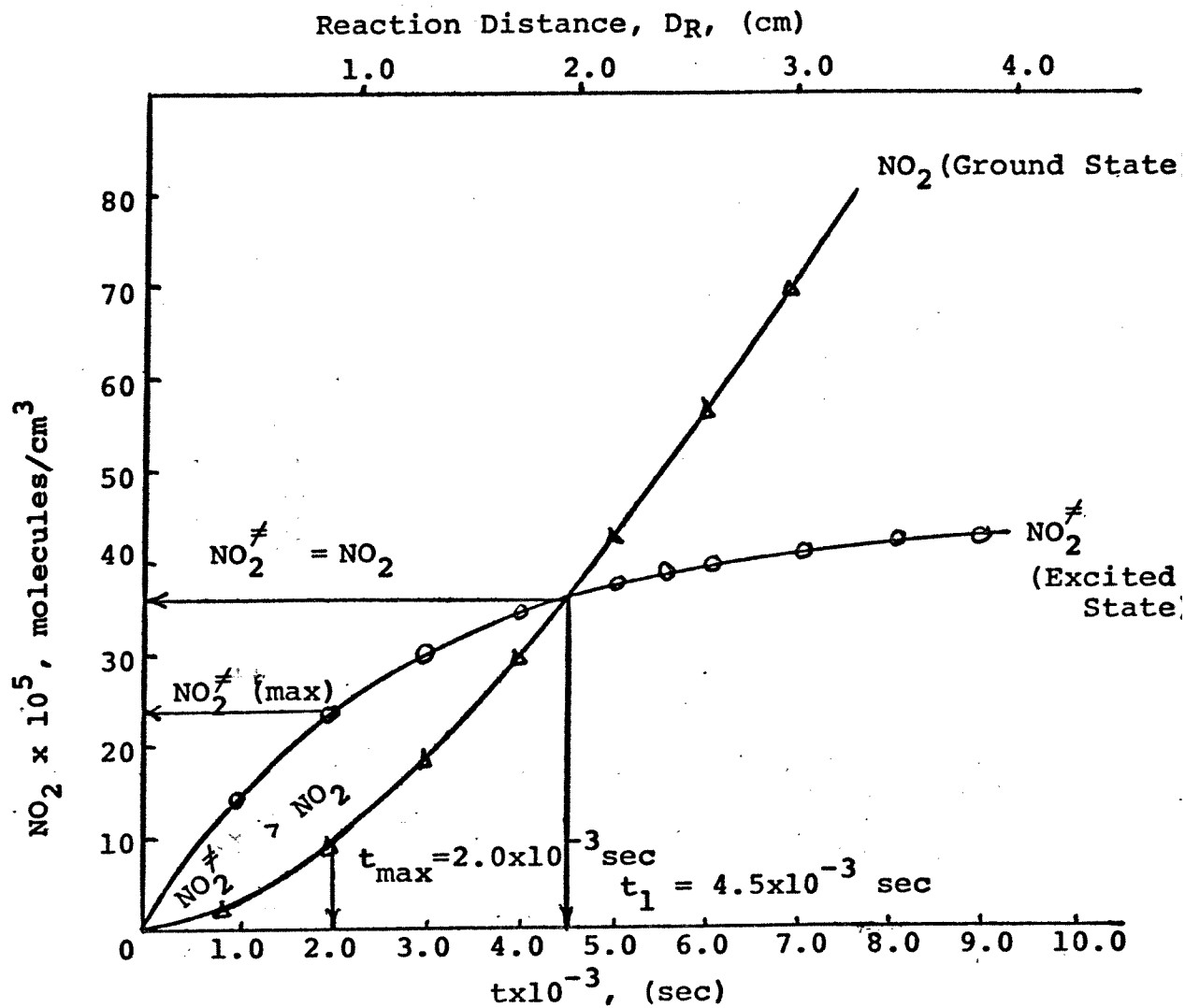


Fig. 14 Time, Distance vs. NO<sub>2</sub> Formation, Excited and Ground States

$$O_3 \text{ (constant)} = 2.0 \times 10^{11} \text{ molecules/cm}^3$$



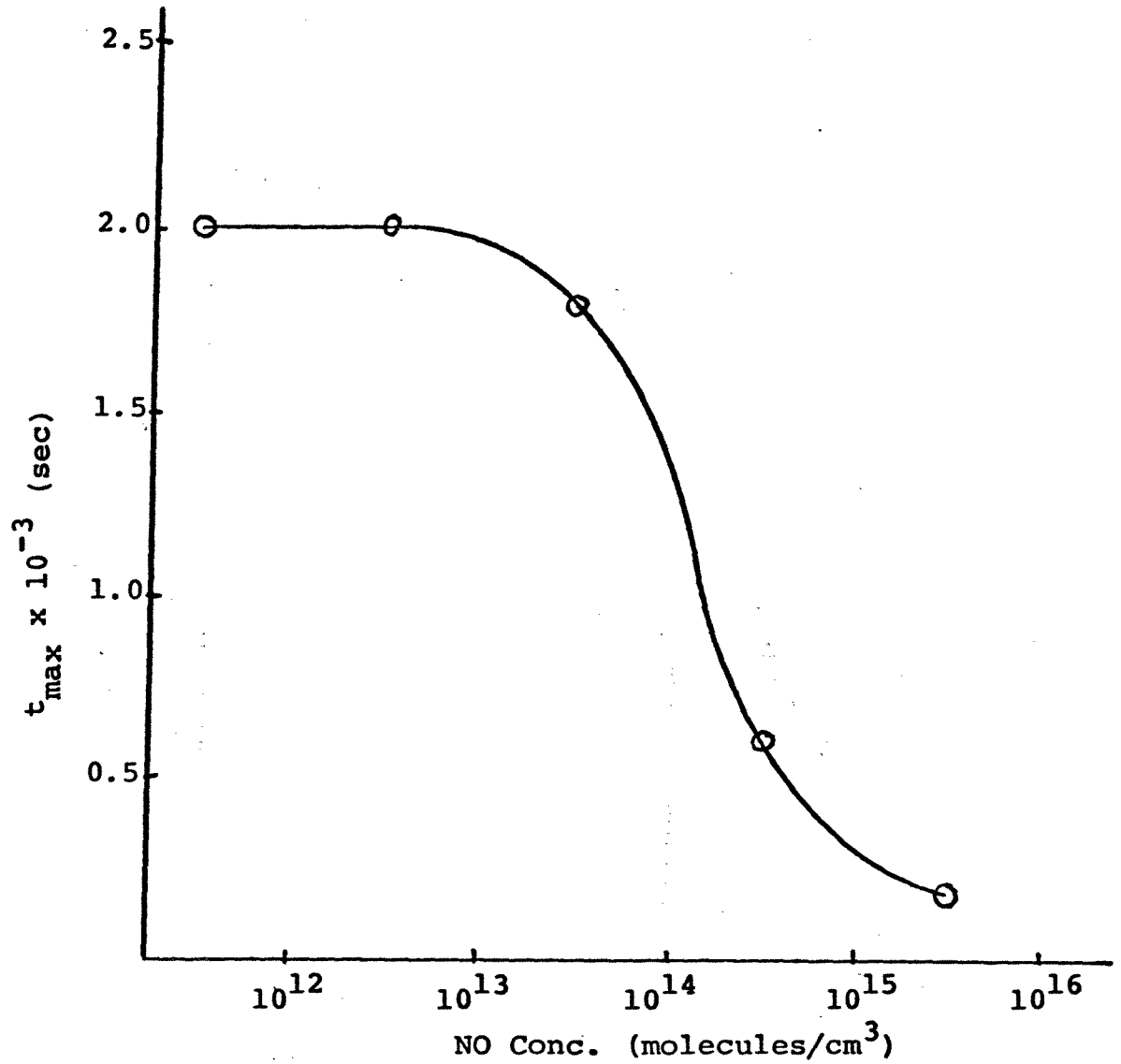


Fig. 15 NO Conc Versus  $t_{\max}$

(Based on Run #6 to Run #10)

$O_3$  (constant) =  $2.0 \times 10^{11}$  molecules/cm<sup>3</sup>

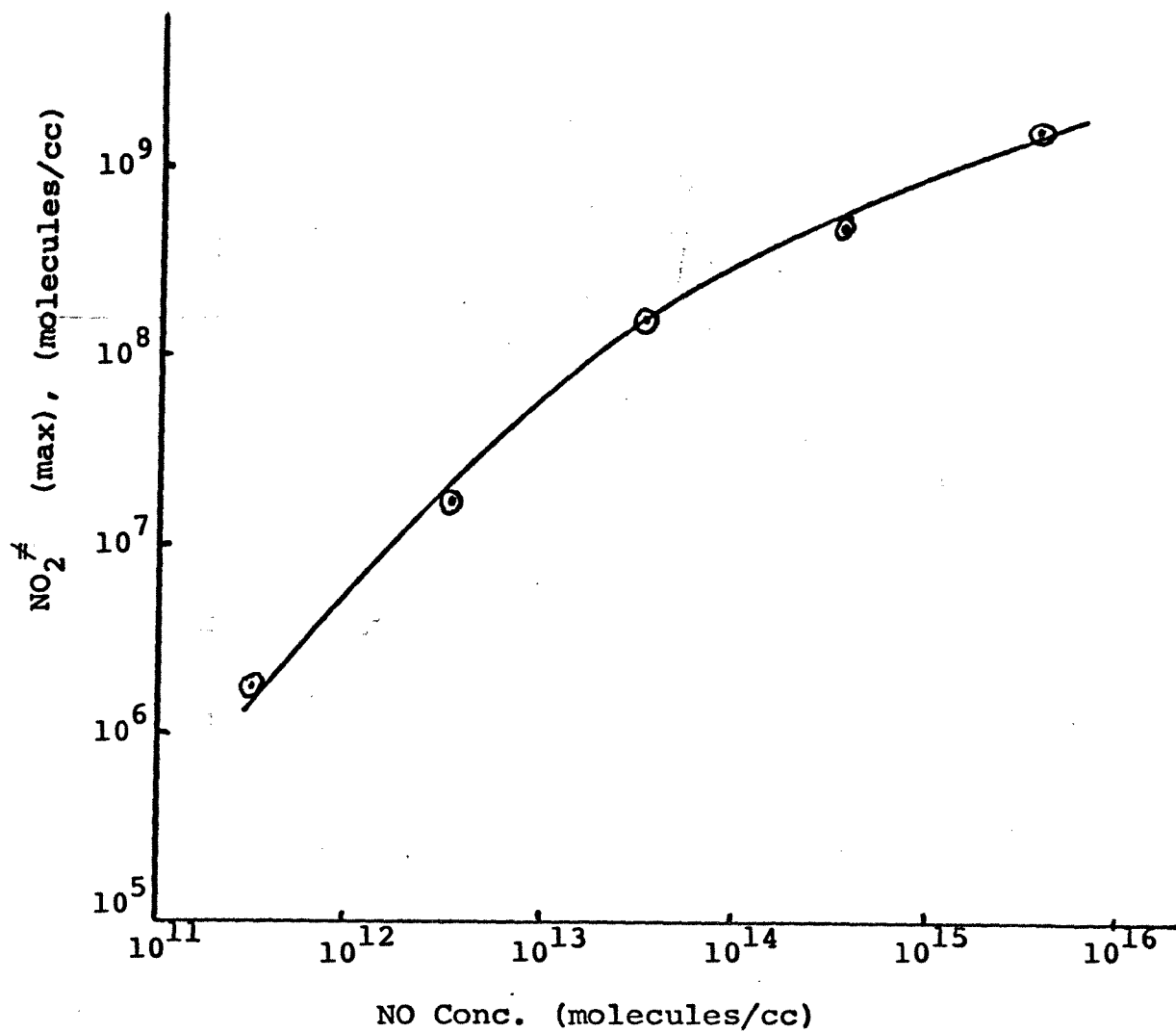


Fig. 16 NO Conc. Versus NO<sub>2</sub><sup>max</sup> (max)

(Based on Run #6 to Run #10)

$$O_3 \text{ (constant)} = 2.0 \times 10^{11} \text{ molecules/cm}^3$$

#### D. Gain Calculations

Light with an intensity  $I$  and frequency  $\nu$  traveling in a given defined  $z$  direction in a reaction chamber containing  $N_1$  and  $N_2$ , where  $N_1$  is the number of atoms or molecules per unit volume ( $\text{cm}^3$ ) which is in a certain energy level (arbitrarily designated as level 1) and  $N_2$  is the number of atoms or molecules per unit volume ( $\text{cm}^3$ ) which is in energy level greater than level 1, may undergo absorption:



where \* means excited state. The light intensity  $I(z)$  is characterized by equation 14:

$$I(z) = I(0)e^{-\alpha z}$$

where  $I(0)$  indicates the light intensity before interaction and  $\alpha$  as the absorption coefficient in  $\text{cm}^{-1}$  and is given for a Gaussian line shape by

$$\alpha = (c^2/4\pi\nu^2\tau) [\ln 2/\pi]^{1/2} (N_1/\Delta\nu) \quad 15$$

In this equation  $c$  is the velocity of light within the material in  $\text{cm}/\text{sec}$ ;  $\tau$ , the fluorescent lifetime of the material in seconds and  $\Delta\nu$  as the half width of the line shape in hertz or cycles/sec.

The same light may undergo amplification by stimulated

emission which is desirable for lasing as shown by equation:

$$I(z) = I(0)e^{gz} \quad 16$$

where  $g$ , the gain coefficient, is given by

$$g = (c^2/4\pi\nu^2\tau) (\ln^2/\pi)^{1/2} (N_2/\Delta\nu) \quad 17$$

Since absorption and stimulated emission are inverse processes, the net effect of passage of light through the  $z$  direction is

$$I(z) = I(0)\exp[(c^2/4\pi\nu^2\tau) (\ln^2/\pi)^{1/2} (1/\Delta\nu) (N_2 - N_1)z] \quad 18$$

If  $N_2 > N_1$  the light intensity will increase as it travels and thus may lead to lasing; if  $N_1 > N_2$ , the light intensity will decrease, which will prevent lasing. For lasing to occur,  $N_2$  must be greater than  $N_1$ , and this situation is known as population inversion. When the material is in thermal equilibrium at temperature  $T$ , the usual population of  $N_1$  and  $N_2$  atoms follow the equation

$$\frac{N_2}{N_1} = e^{-(E_2 - E_1)/kT} \quad 19$$

where  $E_2$  and  $E_1$  corresponds to the energy of the atoms  $N_2$  and  $N_1$ ,  $k$  is Boltzmann's constant equal to  $1.38 \times 10^{-16}$  erg/degree and  $T$  is in absolute temperature. Equation 19 means that  $N_2 < N_1$ , and to obtain laser operation one must upset the thermal equilibrium in some way to produce the unusual situation of a population inversion.

In a laser system, there are inevitable sources of loss which prohibit attainment of population inversion. These losses are: the loss in the output through the two end mirrors, of reflectivities  $R_1$  and  $R_2$  and imperfections in the system. Such losses (imperfections in the optical system) may be characterized by a loss coefficient  $\beta$ , such that the decrease in light intensity is a factor  $e^{-\beta z}$ , a function of the distance  $z$ . [33] Now, using equation 18, the change in light intensity after a round trip through the active medium between two mirrors separated by distance  $L$  involves a factor

$$R_1 R_2 \exp[-2\beta L] \exp[2L(c^2/4\pi\nu^2\tau)(\ln^2/\pi)^{1/2}(N_2 - N_1)/\Delta\nu] \quad 20$$

In order to have a net increase in light intensity, this factor must be greater than unity. Taking the logarithms we have

$$N_2 - N_1 > (4\pi\nu^2\tau\Delta\nu/Lc^2)(\pi/\ln^2)^{1/2}(\beta L - \ln R_1 R_2) \quad 21$$

as the threshold condition -- the minimum population inversion required to sustain laser action in a Gaussian line for a medium with the given properties. [33] Given the wavelength  $\lambda$  as  $3.2 \mu$  or  $3.2 \times 10^{-4}$  cm, the frequency was calculated using the equation

$$\nu = \frac{c}{\lambda} \quad 22$$

which gave  $9.375 \times 10^{13}$ /sec as  $\nu$ . The spread in wavelength,

$\Delta\lambda$  was assumed for  $\nu$  values, one was  $1 \times 10^{-9}$  cm and the other was  $1 \times 10^{-10}$  cm. To calculate for the spread infrequency,  $\Delta\nu$ , assuming small  $\Delta\lambda$ , the equation

$$\Delta\nu = -\left(\frac{c}{\lambda^2}\right)\Delta\lambda \quad 23$$

was used and the values obtained were  $2.93 \times 10^7$  and  $2.93 \times 10^8$   $\nu$ /sec respectively for the two values of  $\Delta\lambda$ s. [34] The fluorescent lifetime was assumed to  $\frac{1}{231}$  or  $4.33 \times 10^{-3}$  sec for IR emission. There were two sets of reflectivities assumed for the mirrors of the cavity. One set was  $R_1$  equaled  $R_2$  equaled 0.90 and the other sets have a value of 0.95.

The loss coefficient  $\beta$  was calculated by using the equation for the loss factor which is:

$$\text{loss factor} = e^{-2\beta z} = e^{-2\beta L}; \quad (L = z) \quad 24$$

where  $L$  stands for the length or distance between the two mirrors. The values given to the loss factor were 0.1, 0.01 and 0.05 which, using the initial laser tube resonant cavity,  $L = 42.4$  cm, gave values of  $\beta$  equal to 0.0272, 0.0553 and  $0.0353 \text{ cm}^{-1}$ . The same values of loss factor were used in the modified laser tube, where the distance was 7.47 cm. The values of  $\beta$  obtained were 0.154, 0.308 and  $0.201 \text{ cm}^{-1}$ , see Table 11.

All the values of  $\nu$ ,  $\tau$ ,  $\Delta\nu$ ,  $L$ ,  $\beta$ ,  $R_1$ ,  $R_2$  and assuming

$c$  as the velocity of light in the material to be equal to velocity of light in vacuo were substituted into equation 21. The results of such calculations gave the required minimum population inversion for lasing in the cavity,  $N_2 > N_1$ , see Tables 12, 13 and 14 for initial laser tube calculations and Tables 15, 16 and 17 for the modified laser tube calculations. The tables for both initial and modified laser tubes showed that the required minimum population inversion were fully satisfied,  $N_2 > N_1$  at different values of  $\beta$  and variables. The calculation for the actual population inversion was done in the Kinetic section, part C. The results of the gain calculations as well as the kinetic aspect are further discussed in Section IV, Results and Discussion.

TABLE 11 $\beta$  Values for Initial and Modified Laser Tubes

	<u>Initial Laser Tube</u>	<u>Modified Laser Tube</u>
	<u><math>\beta, \text{cm}^{-1}</math></u>	<u><math>\beta, \text{cm}^{-1}</math></u>
$e^{-2\beta L} = 0.1$	0.0272	0.154
$e^{-2\beta L} = 0.01$	0.0553	0.308
$e^{-2\beta L} = 0.05$	0.0353	0.201

$\beta$  = loss coefficient for the imperfections in the system

$e^{-2\beta L}$  = a factor for the decrease in light intensity as it travels back and forth (2L).



TABLE 12

$N_2 - N_1$  for Initial Laser Tube,  $\beta = 0.0272 \text{ cm}^{-1}$

Variables & Constants	1	2	3	4
$\lambda$ (cm)	$3.2 \times 10^{-4}$	$3.2 \times 10^{-4}$	$3.2 \times 10^{-4}$	$3.2 \times 10^{-4}$
$\nu$ (/sec)	$9.375 \times 10^{13}$	$9.375 \times 10^{13}$	$9.375 \times 10^{13}$	$9.375 \times 10^{13}$
$\Delta\lambda$ (cm)	$1 \times 10^{-9}$	$1 \times 10^{-10}$	$1 \times 10^{-9}$	$1 \times 10^{-10}$
$\Delta\nu$ (/sec)	$2.93 \times 10^8$	$2.93 \times 10^7$	$2.93 \times 10^8$	$2.93 \times 10^7$
$\tau$ (sec)	$4.33 \times 10^{-3}$	$4.33 \times 10^{-3}$	$4.33 \times 10^{-3}$	$4.33 \times 10^{-3}$
$L$ (cm)	42.4	42.4	42.4	42.4
$R_1$	0.90	0.90	0.95	0.95
$R_2$	0.90	0.90	0.95	0.95
$\beta$ ( $\text{cm}^{-1}$ )	0.0272	0.0272	0.0272	0.0272
$N_2 - N_1$ ( $\frac{\text{molecules}}{\text{cm}^3}$ )	$1.06 \times 10^{13}$	$1.06 \times 10^{12}$	$9.8 \times 10^{12}$	$9.8 \times 10^{11}$

TABLE 13

$N_2 - N_1$  for Initial Laser Tube,  $\beta = 0.0543 \text{ cm}^{-1}$

Variables & Constants	5	6	7	8
$\lambda$ (cm)	$3.2 \times 10^{-4}$	$3.2 \times 10^{-4}$	$3.2 \times 10^{-4}$	$3.2 \times 10^{-4}$
$\nu$ (~ /sec)	$9.375 \times 10^{13}$	$9.375 \times 10^{13}$	$9.375 \times 10^{13}$	$9.375 \times 10^{13}$
$\Delta\lambda$ (cm)	$1 \times 10^{-9}$	$1 \times 10^{-10}$	$1 \times 10^{-9}$	$1 \times 10^{-10}$
$\Delta\nu$ ( /sec)	$2.93 \times 10^8$	$2.93 \times 10^7$	$2.93 \times 10^8$	$2.93 \times 10^7$
$\tau$ (sec)	$4.33 \times 10^{-3}$	$4.33 \times 10^{-3}$	$4.33 \times 10^{-3}$	$4.33 \times 10^{-3}$
L (cm)	42.4	42.4	42.4	42.4
$R_1$	0.90	0.90	0.95	0.95
$R_2$	0.90	0.90	0.95	0.95
$\beta$ ( $\text{cm}^{-1}$ )	0.0543	0.0543	0.0543	0.0543
$N_2 - N_1$ ( $\frac{\text{molecules}}{\text{cm}^3}$ )	$1.96 \times 10^{13}$	$1.96 \times 10^{12}$	$1.88 \times 10^{13}$	$1.88 \times 10^{12}$

TABLE 14

$N_2 - N_1$  for Initial Laser Tube,  $\beta = 0.0353 \text{ cm}^{-1}$

Variables & Constants	9	10	11	12
$\lambda$ (cm)	$3.2 \times 10^{-4}$	$3.2 \times 10^{-4}$	$3.2 \times 10^{-4}$	$3.2 \times 10^{-4}$
$\nu$ (~/sec)	$9.375 \times 10^{13}$	$9.375 \times 10^{13}$	$9.375 \times 10^{13}$	$9.375 \times 10^{13}$
$\Delta\lambda$ (cm)	$1 \times 10^{-9}$	$1 \times 10^{-10}$	$1 \times 10^{-9}$	$1 \times 10^{-10}$
$\Delta\nu$ (~/sec)	$2.93 \times 10^8$	$2.93 \times 10^7$	$2.93 \times 10^8$	$2.93 \times 10^7$
$\tau$ (sec)	$4.33 \times 10^{-3}$	$4.33 \times 10^{-3}$	$4.33 \times 10^{-3}$	$4.33 \times 10^{-3}$
$L$ (cm)	42.4	42.4	42.4	42.4
$R_1$	0.90	0.90	0.95	0.95
$R_2$	0.90	0.90	0.95	0.95
$\beta$ ( $\text{cm}^{-1}$ )	0.0353	0.0353	0.0353	0.0353
$N_2 - N_1$ ( $\frac{\text{molecules}}{\text{cm}^3}$ )	$1.33 \times 10^{13}$	$1.33 \times 10^{12}$	$1.25 \times 10^{13}$	$1.25 \times 10^{12}$

TABLE 15

$N_2 - N_1$  for Modified Laser Tube,  $\beta = 0.154 \text{ cm}^{-1}$

Variables & Constants	13	14	15	16
$\lambda$ (cm)	$3.2 \times 10^{-4}$	$3.2 \times 10^{-4}$	$3.2 \times 10^{-4}$	$3.2 \times 10^{-4}$
$\nu$ (~ / sec)	$9.375 \times 10^{13}$	$9.375 \times 10^{13}$	$9.375 \times 10^{13}$	$9.375 \times 10^{13}$
$\Delta\lambda$ (cm)	$1 \times 10^{-9}$	$1 \times 10^{-10}$	$1 \times 10^{-9}$	$1 \times 10^{-10}$
$\Delta\nu$ (~ / sec)	$2.93 \times 10^8$	$2.93 \times 10^7$	$2.93 \times 10^8$	$2.93 \times 10^7$
$\tau$ (sec)	$4.33 \times 10^{-3}$	$4.33 \times 10^{-3}$	$4.33 \times 10^{-3}$	$4.33 \times 10^{-3}$
$L$ (cm)	7.47	7.47	7.47	7.47
$R_1$	0.90	0.90	0.95	0.95
$R_2$	0.90	0.90	0.95	0.95
$\beta$ ( $\text{cm}^{-1}$ )	0.154	0.154	0.154	0.154
$N_2 - N_1$ ( $\frac{\text{molecules}}{\text{cm}^3}$ )	$6.04 \times 10^{13}$	$6.04 \times 10^{12}$	$5.56 \times 10^{13}$	$5.56 \times 10^{12}$

TABLE 16

$N_2 - N_1$  for Modified Laser Tube,  $\beta = 0.308 \text{ cm}^{-1}$

Variables & Constants	17	18	19	20
$\lambda$ (cm)	$3.2 \times 10^{-4}$	$3.2 \times 10^{-4}$	$3.2 \times 10^{-4}$	$3.2 \times 10^{-4}$
$\nu$ (~ / sec)	$9.375 \times 10^{13}$	$9.375 \times 10^{13}$	$9.375 \times 10^{13}$	$9.375 \times 10^{13}$
$\Delta\lambda$ (cm)	$1 \times 10^{-9}$	$1 \times 10^{-10}$	$1 \times 10^{-9}$	$1 \times 10^{-10}$
$\Delta\nu$ (~ / sec)	$2.93 \times 10^8$	$2.93 \times 10^7$	$2.93 \times 10^8$	$2.93 \times 10^7$
$\tau$ (sec)	$4.33 \times 10^{-3}$	$4.33 \times 10^{-3}$	$4.33 \times 10^{-3}$	$4.33 \times 10^{-3}$
$L$ (cm)	7.47	7.47	7.47	7.47
$R_1$	0.90	0.90	0.95	0.95
$R_2$	0.90	0.90	0.95	0.95
$\beta$ ( $\text{cm}^{-1}$ )	0.308	0.308	0.308	0.308
$N_2 - N_1$ ( $\frac{\text{molecules}}{\text{cm}^3}$ )	$1.11 \times 10^{14}$	$1.11 \times 10^{13}$	$1.06 \times 10^{14}$	$1.06 \times 10^{13}$

TABLE 17

$N_2 - N_1$  for Modified Laser Tube,  $\beta = 0.201 \text{ cm}^{-1}$

Variables & Constants	17	18	19	20
$\lambda$ (cm)	$3.2 \times 10^{-4}$	$3.2 \times 10^{-4}$	$3.2 \times 10^{-4}$	$3.2 \times 10^{-4}$
$\nu$ (~ / sec)	$9.375 \times 10^{13}$	$9.375 \times 10^{13}$	$9.375 \times 10^{13}$	$9.375 \times 10^{13}$
$\Delta\lambda$ (cm)	$1 \times 10^{-9}$	$1 \times 10^{-10}$	$1 \times 10^{-9}$	$1 \times 10^{-10}$
$\Delta\nu$ (~ / sec)	$2.93 \times 10^{18}$	$2.93 \times 10^7$	$2.93 \times 10^8$	$2.93 \times 10^7$
$\tau$ (sec)	$4.33 \times 10^{-3}$	$4.33 \times 10^{-3}$	$4.33 \times 10^{-3}$	$4.33 \times 10^{-3}$
L (cm)	7.47	7.47	7.47	7.47
$R_1$	0.90	0.90	0.95	0.95
$R_2$	0.90	0.90	0.95	0.95
$\beta$ ( $\text{cm}^{-1}$ )	0.201	0.201	0.201	0.201
$N_2 - N_1$ ( $\frac{\text{molecules}}{\text{cm}^3}$ )	$7.59 \times 10^{13}$	$7.59 \times 10^{12}$	$7.11 \times 10^{13}$	$7.11 \times 10^{12}$

#### IV. RESULTS AND DISCUSSION

##### A. Initial Laser Tube

The results of the initial laser tube experiments are tabulated in Table 2. No definite strong lasing was observed, although weak signals indicative of lasing were periodically observed. These were, however, not completely reproducible.

A strong chemiluminescence (red glow) was observed during the reaction of NO with O<sub>3</sub> with the maximum near the ozone inlet and moving gradually downstream near the NO inlet as the NO and Ar mixture in the flask became depleted. The chemiluminescence intensity was proportional to the NO concentration in the reactor indicating the reaction was occurring at a faster rate.

The amount of gas available in the one-liter flask was calculated using the ideal gas law,  $PV = nRT$ . At one atmosphere pressure and a temperature of 20°C (293°K), the total molecules available per cm<sup>3</sup> was

$$(NO + Ar) = \frac{n}{V} = \frac{P}{RT}$$
$$= \frac{1 \text{ atm}}{0.082 \frac{\text{atm-li}}{\text{mole-}^\circ\text{K}}} \times \frac{1 \text{ li}}{1000 \text{ cm}^3} \times \frac{1}{293^\circ\text{K}} \times \frac{6.02 \times 10^{23} \text{ molecules}}{\text{mole}}$$

$$(NO + Ar) = 2.51 \times 10^{19} \text{ molecules/cm}^3$$

This was the amount of NO/Ar in the one-liter flask used per experimental run. The experimental runs composed of different NO concentrations: 25%, 50%, 75%, 85%, 95% and 100% by volume of NO, corresponding to  $6.275 \times 10^{18}$ ,  $1.255 \times 10^{19}$ ,  $1.88 \times 10^{19}$ ,  $2.13 \times 10^{19}$ ,  $2.38 \times 10^{19}$  and  $2.51 \times 10^{19}$  molecules/cm<sup>3</sup>.

There was no flowmeter available at the time so that the flows were determined by calculation using evacuation time of the Ar/NO flask. The one-liter flask was completely exhausted within two minutes, giving the average flow rate of

$$\frac{1000 \text{ cm}^3}{2 \text{ min}} \times \frac{1 \text{ min}}{60 \text{ sec}} = 8.33 \frac{\text{cm}^3}{\text{sec}}$$

The needle valve on the Ar/NO inlet was constantly adjusted to maintain a constant pressure in the flow tube and thus keeping the flow relatively constant. The experiments were carried out in such a manner that the argon flow sweeping the ozone out of the low temperature matrix trap could be varied from 0.5 to 2.0 cm<sup>3</sup>/sec (ATP) at pressure of 0.427 torr. Occasionally, during the experiments, particularly at the end (see Table 7), the argon flow was increased, i.e. 16.0 torr pressure. The amount of ozone flow vary at low pressure from 0.05 to 0.20 cm<sup>3</sup>/sec, assuming the argon picked up ozone to a ten percent level in the mix.<sup>[18]</sup> At higher pressures of 16.0 torr pressure, (ozone picked up at 10% level), giving 1.6 torr partial pressure [O<sub>3</sub>].

Investigation of the distance from the reactant inlet (NO), linear velocity and the kinetic calculations revealed that the



desired reaction products (excited  $\text{NO}_2^{\neq}$ ) was being rapidly lost to vibrational de-excitation in the initial reactor. This distance, called reaction distance, ( $D_R$ ), was 24.2 cm in the initial laser tube and only 2.68 cm in the modified laser tube. In Table 3, the linear flow velocity was calculated at different volumetric flow rates and pressures. Residence time ( $t_R$ ) or reaction time is the length of time the gas reactants spend in the laser tube reactor. Appendix B includes the results of a typical kinetic run of No. 6 (see Table 9 for results of the summary of the kinetic run of No. 6). The concentration of the excited state  $\text{NO}_2^{\neq}$  and the ground state  $\text{NO}_2^{\circ}$  at different times in this run were calculated at varied reaction distance,  $D_R$ , reaction time,  $t_R$ , and tabulated in Table 18. The reaction time  $t_R$ , was calculated from the reciprocal of the typical velocity of the gas molecules in the reactor at 0.65 torr (Table 7) and volumetric flow rate of  $1.51 \text{ cm}^3/\text{sec}$  (Table 3),  $1/478.6 \text{ cm/sec}$  multiply by the reaction distance:

$$t_R = \frac{1}{478.6 \frac{\text{cm}}{\text{sec}}} \times D_R \text{ (cm)} = 0.002 \text{ sec reaction time}$$

The difference,  $(\text{NO}_2^{\neq} - \text{NO}_2^{\circ})$  determines the population inversion in time (distance). A negative sign indicates that the ground state population is larger than the excited state. An average of this difference  $(\text{NO}_2^{\neq} - \text{NO}_2^{\circ})$  in the initial laser tube was calculated to be  $-33.06 \times 10^6 \text{ molecules/cm}^3$ . Thus, there were no population inversion. This means that population inversion did not exist in the initial laser tube and prevented

lasing. Examination of Table 18 and Figure 14 showed that population inversion ( $\text{NO}_2^{\neq} > \text{NO}_2^{\circ}$ ) occurred at the start of the reaction and continued to a reaction distance of 2.25 cm and reaction time of 4.5 m sec.

#### B. Modified Laser Tube

The modified laser tube which had a reaction distance of 2.63 cm was calculated to have an average population inversion of  $1.32 \times 10^6$  molecules/cm<sup>3</sup> (see Table 18) and therefore lasing should occur.

The maximum population inversion was the maximum difference between the excited state and the ground state  $(\text{NO}_2^{\neq} - \text{NO}_2^{\circ})_{\text{max}}$ . This occurred at reaction distance of 1 cm downstream and at reaction time of ca 2 m sec., see Figure 14. To emphasize this point, we used the symbol  $t_{\text{max}}$  as maximum reaction time and  $(\text{NO}_2^{\neq})_{\text{max}}$  as the maximum concentration of the excited state at maximum population inversion. It is desirable to have a high population inversion for lasing.

It was shown by the kinetics computer program that a population inversion was achieved in the modified laser tube. It was important to determine whether the amount of radiation coming out of the laser tube was sufficient for detection and displayed on the oscilloscope.

Assuming that the laser soon reaches optimum output from gradual build-up of photons in cavity to stimulate emission for a continuous laser. This optimum is a steady state condi-

TABLE 18

Population Inversion, Reaction Distance & Residence Time in a Reactor Tube

Reaction Distance $D_R$ (cm)	Reaction Time $t_R$ (msec)	Concentration	Concentration	$NO_2^{\neq} - NO_2^{\circ}$ ( $\frac{\text{molecules}}{\text{cm}^3}$ ) $\times 10^6$	Population Inversion Yes, No
		Excited State $NO_2^{\neq}$ ( $\frac{\text{molecules}}{\text{cm}^3}$ ) $\times 10^6$	Ground State $NO_2^{\circ}$ ( $\frac{\text{molecules}}{\text{cm}^3}$ ) $\times 10^6$		
0	0	0	0	0	No
1	2	2.36	0.86	1.50	Yes, Max
2	4	3.47	2.97	0.50	Yes
3	6	4.00	5.65	-1.65	No
4	8	4.26	8.62	-4.36	No
5	10	4.38	11.7	-7.32	No
6	12	4.43	14.9	-10.47	No
7	14	4.46	18.1	-13.64	No
8	16	4.47	21.3	-16.83	No
9	18	4.48	24.5	-20.02	No
10	20	4.48	27.7	-23.22	No
11	22	4.48	30.9	-26.42	No
12	24	4.48	34.2	-28.02	No
13	26	4.48	37.4	-32.92	No
14	28	4.48	40.6	-36.12	No
15	30	4.48	43.8	-39.32	No
16	32	4.48	47.0	-42.52	No
17	34	4.48	50.2	-45.72	No
18	36	4.48	53.5	-49.02	No
19	38	4.48	56.7	-52.22	No
20	40	4.48	59.9	-55.42	No
21	42	4.48	63.1	-58.62	No
22	44	4.48	66.3	-61.82	No
23	46	4.48	69.5	-65.02	No
24	48	4.48	72.7	-68.22	No
29.2	48.4	4.48	73.98	-69.50	No

tion where  $(NO_2^\# - NO_2^\circ)_{\text{steady state}} < (NO_2^\# - NO_2^\circ)_{\text{avg}}$  of the kinetic calculations. The difference in the population inversion between the kinetic calculations and the population inversion where gain is equal to 1.0 will give us the amount of photons in the stimulated emission (steady state condition). Equation 25 gives the gain calculation as:

$$I(z) = I(0)R_1R_2 \exp^{-2\beta L} \exp[2L(c^2/4\pi\nu^2\tau) [\ln 2/\pi]^{1/2} \frac{(NO_2^\# - NO_2^\circ)}{\Delta\nu}]$$

for 1 transversal (back and forth). The number of transversal (use  $T_N$  as symbol) was calculated as:

$$\begin{aligned} T_N = \text{No. of transversal} &= \frac{\text{Average } A_{\text{tube}} - A_{\text{hole}}}{A_{\text{hole}}}, \quad A = \text{Cross-sectional area} \\ &= \frac{\pi r_{\text{tube}}^2 - \pi r_{\text{hole}}^2}{\pi r_{\text{hole}}^2} = \frac{r_{\text{tube}}^2 - r_{\text{hole}}^2}{r_{\text{hole}}^2} \\ &= \frac{(\frac{2.68}{2} \text{ cm})^2 - (\frac{0.18}{2} \text{ cm})^2}{(\frac{0.18}{2} \text{ cm})^2} \end{aligned}$$

$$\therefore T_N = 224.6$$

If we let G as the gain factor, equation 25 will be:

$$I(z) = I(o)G, \text{ where}$$

$$G = T_N R_1 R_2 \exp^{-2\beta L} \exp[2L(c^2/4\pi\nu^2\tau) [\ln 2/\pi]^{1/2} (NO_2^\# - NO_2^\circ)/\Delta\nu]$$

$$R_1 = 1.000$$

$$R_2 = 0.976$$

$$\exp^{-2\beta L} = 0.001$$

$$\beta = 0.46$$

$$l = 7.47 \text{ cm}$$

$$c = 3 \times 10^{10} \text{ cm/sec}$$

$$v = 9.375 \times 10^{13} \text{ ~}/\text{sec}$$

$$\tau = 4.33 \times 10^{-3} \text{ sec}$$

$$\lambda = 3.2 \times 10^{-4} \text{ cm}$$

$$\Delta\lambda = 1 \times 10^{-11} \text{ cm and}$$

$$\Delta\nu = \frac{c}{\lambda^2}(\Delta\lambda) = \frac{3 \times 10^{10}}{(3.2 \times 10^{-4})^2} (1 \times 10^{-11})$$

$$\therefore \Delta\nu = 2.93 \times 10^6 \text{ ~}/\text{sec}$$

In a steady state, C.W. laser  $G = 1$  is a requirement, thus the population inversion at this condition was calculated after substituting the variables above as:

$$\frac{(\text{NO}_2^{\neq} - \text{NO}_2^{\circ})}{\text{Gain } 1.0} = 3.33 \times 10^{11} \frac{\text{molecules}}{\text{cm}^3}$$

the ozone concentrations at low pressures of 0.0427 torr will give:

$$[\text{O}_3] = \frac{n}{V} = \frac{P}{RT} = \frac{0.0427 \text{ torr} \times \frac{1 \text{ atm}}{760 \text{ torr}}}{0.082 \frac{\text{atm-li}}{\text{mole-}^\circ\text{K}}} \times \frac{1 \text{ li}}{1000 \text{ cm}^3} \times \frac{1}{293^\circ\text{K}}$$

$$\times 6.02 \times 10^{23} \frac{\text{molecules}}{\text{mole}}$$

$$[\text{O}_3]_{\text{low pressure}} = 1.41 \times 10^{15} \frac{\text{molecules}}{\text{cm}^3}$$

and at high pressure of 1.6 torr:

$$[\text{O}_3]_{\text{high pressure}} = 5.3 \times 10^{16} \frac{\text{molecules}}{\text{cm}^3}$$

Adjusting the population inversion in the kinetic calculations we have two conditions of pressure for these calculations.

(a) At low pressure (0.0427 torr):

$$(\text{NO}_2^{\neq} - \text{NO}_2^{\circ})_{\text{ave}} = 1.32 \times 10^6 \times \frac{1.41 \times 10^{15}}{2.0 \times 10^{11}} = 9.3 \times 10^9 \frac{\text{molecules}}{\text{cm}^3}$$

(b) At high pressure (1.5 torr):

$$(\text{NO}_2^{\neq} - \text{NO}_2^{\circ})_{\text{ave}} = 1.32 \times 10^6 \times \frac{5.3 \times 10^{16}}{2.0 \times 10^{11}} = 3.5 \times 10^{11} \frac{\text{molecules}}{\text{cm}^3}$$

These values compared to the value obtained in the gain calculation which was equal to:

$$(\text{NO}_2^{\neq} - \text{NO}_2^{\circ})_{\text{gain} = 1.0} = 3.33 \times 10^{11} \frac{\text{molecules}}{\text{cm}^3}$$

showed that at low pressures,  $(\text{NO}_2^{\neq} - \text{NO}_2^{\circ})_{\text{avg}}$  is less than  $(\text{NO}_2^{\neq} - \text{NO}_2^{\circ})_{\text{gain} = 1.0}$  and lasing will probably not occur. Whereas, at high pressures, the difference between the population inversion gives the photons emitted due to stimulated emission at steady state:

$$\begin{aligned} \frac{\text{photons}}{\text{sec}} &= [\text{NO}_2^{\neq} - \text{NO}_2^{\circ}]_{\text{ave}}^{\text{high pressure}} - [\text{NO}_2^{\neq} - \text{NO}_2^{\circ}]_{\text{gain} = 1.0} \\ &= 3.5 \times 10^{11} - 3.33 \times 10^{11} \\ &= 1.7 \times 10^{10} \frac{\text{photons}}{\text{sec}} \end{aligned}$$

This converted into power where the energy in erg per photon was calculated as follows:

$$\text{photon} = h\nu \quad , \quad \nu = 9.375 \times 10^{13} \text{ ~}/\text{sec}$$

and  $h = 6.62 \times 10^{-27} \text{ erg-sec}$  (Planck's constant) so,

$$\begin{aligned} \text{one photon} &= 6.62 \times 10^{-27} \times 9.375 \times 10^{13} \\ &= 6.2 \times 10^{-13} \text{ erg} \end{aligned}$$

The power before hitting the detector:

$$\begin{aligned} \text{Power} &= 1.7 \times 10^{10} \frac{\text{photons}}{\text{sec}} \times 6.2 \times 10^{-13} \frac{\text{erg}}{\text{photon}} \times \frac{1 \text{ joule}}{10^7 \text{ ergs}} \\ &\quad \times \frac{1 \text{ watt}}{1 \frac{\text{joule}}{\text{sec}}} \end{aligned}$$

$$\text{Power} = 1.05 \times 10^{-9} \text{ watt}$$

This power was being blocked by the chopper part of the time so that only 45% of the radiation was allowed to pass. The windows of the reactor tube were not in Brewster angle and a 4% maximum loss was anticipated. The detectors have a spectral response of 321 volt/watt and amplification factor of  $10^5$ . The output mirror was only 2.4% transmission. All of this, when taken into consideration, will give a voltage signal on the oscilloscope of:

$$\begin{aligned} \text{Voltage signal} &= 1.05 \times 10^{-9} \text{ watt} \times 0.45 \times 0.96 \times .024 \\ &\quad \times 10^5 \times \frac{321 \text{ volt}}{\text{watt}} \times \frac{10^3 \text{ mV}}{1 \text{ volt}} \end{aligned}$$

Therefore:

$$\text{Voltage signal} = 0.35 \text{ mV}$$

A 25 mV signal could just be observed and is considered the minimal detectable signal in the oscilloscope. This voltage

signal, as calculated, could not be detected and may be the reason why there were no definite lasing experienced in this modified laser tube except for several occasions which showed signs of weak, sporadic signals, but were not consistently reproducible.

An alternative calculation of the power output showed the cavity not reaching steady state can be performed as follows (note this calculation is not as accurate as previous calculations):

From the data in the first calculation, we have

$$I(z) = I(o) T_N G$$

where  $T_N$  = no. of transversals = 224.6

$G$  = gain factor for 1 transversal using same variables as before:

$$= R_1 R_2 \exp(-2\beta L) \exp[2L(c^2/4\pi v^2 \tau) [(ln^2)/\pi]^{1/2} (NO_2^\circ - NO_2^\circ)_{ave}/\Delta v]$$

Substituting the values of the variables, we obtained,

$$T_N G = 1.06$$

$$I(z) = I(o) (1.06)$$

To find  $I(o)$ , we used equation 1B:

$$NO_2^\circ \frac{k_{1B}}{k_{1B}} NO_2^\circ + hv$$

and

$$\frac{d(hv)}{dt} = k_{1B} [NO_2^\circ], \text{ so}$$

$$hv = k_{1B} \left[ [NO_2^\circ]_{orig} - [NO_2^\circ]_t \right]$$



where  $[\text{NO}_2^\ddagger]_{\text{orig}}$  was the original concentration of  $\text{NO}_2^\ddagger$  before photon emission and  $[\text{NO}_2^\ddagger]_t$  was the concentration of  $\text{NO}_2^\ddagger$  after a time  $t$ .  $k_{1B}$  was equal to  $230 \text{ sec}^{-1}$ . The  $[\text{NO}_2^\ddagger]_{\text{orig}}$  was  $2.36 \times 10^6 \text{ molecules/cm}^3$ , which was the average  $\text{NO}_2^\ddagger$  at reaction time of 4.25 m sec and reaction distance of 2.68 cm. Considering spontaneous emission, only:

$$[\text{NO}_2^\ddagger]_t = [\text{NO}_2^\ddagger]_{\text{orig}} \exp^{-k_{1B}t} \quad 28$$

Ref. [35]. Substituting the values of  $[\text{NO}_2^\ddagger]_{\text{orig}}$ ,  $k_{1B}$  and  $t$  (0.002 sec) in equation (28):

$$[\text{NO}_2^\ddagger] = 1.49 \times 10^6 \text{ molecules/cm}^3.$$

Now we can calculate for  $h\nu$  by substituting all the variables in equation (27):

$$\begin{aligned} h\nu &= 230 [2.36 \times 10^6 - 1.49 \times 10^6] \\ &= 2.0 \times 10^8 \frac{\text{photons}}{\text{cm}^3 - \text{sec}} \end{aligned}$$

This was the calculated intensity of the radiation produced by the reaction, per  $4\pi$  steradians. The emission responsible for the stimulated process was confined only to the solid angles from the center of the resonant cavity into the two mirrors (assuming the reaction was in the center of the resonant cavity). The center of the resonant cavity was  $\frac{7.47}{2} = 3.74 \text{ cm}$ . Solid angle of the 100% reflectance mirror,  $\Omega_1$ , was calculated as:

$$\Omega_1 = \frac{A_1}{r_1^2} = \frac{5.64 \text{ cm}^2}{(3.74 \text{ cm})^2} = 0.403 \text{ steradians}$$

where

$A_1$  = cross sectional area of the mirror

$r_1$  = the distance from the center of the resonant cavity to the mirror.

The solid angle of the 97.6% reflectance mirror,  $\Omega_2$ , was calculated as:

$$\Omega_2 = \frac{A_1}{r_1^2} - \frac{A_{\text{hole}}}{r_1^2} = \frac{5.64 \text{ cm}^2 - 0.025 \text{ cm}^2}{(3.74 \text{ cm})^2} = 0.401 \text{ steradians}$$

The sum of the solid angles  $\Omega_1$  and  $\Omega_2$  is equal to  $0.403 + 0.401 = 0.801$  steradians. The spherical solid angle was calculated as

$$\begin{aligned} \Omega_{\text{spherical}} &= \frac{A_{\text{sphere}}}{r_1^2} \\ &= \frac{4\pi r_1^2}{r_1^2} \\ &= 4\pi \text{ steradians} \end{aligned}$$

So the fraction of the solid angle,  $f$ , which was effective for lasing was

$$f = \frac{\Omega_1 + \Omega_2}{\Omega_{\text{spherical}}} = \frac{0.801}{4\pi} = 0.064$$

One photon is equal to  $6.2 \times 10^{-13}$  erg as calculated previously.

So the total energy in ergs:

$$E = 6.2 \times 10^{-13} \frac{\text{erg}}{\text{photon}} \times 2.0 \times 10^8 \frac{\text{photon}}{\text{cm}^3 \cdot \text{sec}} \times 22.3 \text{ cm}^3 = 2.8 \times 10^{-3} \frac{\text{erg}}{\text{sec}}$$

The power will be:

$$\text{Power} = 2.8 \times 10^{-3} \frac{\text{erg}}{\text{sec}} \times (\text{Gain}) \times f = 2.8 \times 10^{-3} \times 1.06 \times 0.064$$

$$\text{Power} = 1.9 \times 10^{-4} \frac{\text{erg}}{\text{sec}}$$

But the radiation coming out of the reactor tube was only a fraction of the ratio between the cross-sectional areas of the small hole and the reactor tube. The chopper, in addition, was blocking the radiation 55% of the time. The windows were not at Brewster angle and a 4% loss was assumed. The detector amplifies the signal by a factor of  $10^5$  and its spectral response was 321 volt/watt. The final voltage signal in millivolt then was:

$$\text{Voltage signal} = I(z) \times (\text{flat mirror transmission}) \times \frac{1 \text{ joule}}{1 \times 10^7 \text{ ergs}}$$

$$\times \frac{1 \text{ watt}}{1 \frac{\text{joule}}{\text{sec}}} \times 0.45 \times 0.96 \times 10^5 \times 321 \frac{\text{volt}}{\text{watt}} \times \frac{10^3 \text{ mV}}{1 \text{ volt}}$$

$$= 1.9 \times 10^{-4} \frac{\text{erg}}{\text{sec}} \times 0.024 \times \frac{1 \text{ joule}}{1 \times 10^7 \text{ ergs}} \times \frac{1 \text{ watt}}{1 \frac{\text{joule}}{\text{sec}}} \times 0.45 \times 0.96$$

$$\times 10^5 \times 321 \frac{\text{volt}}{\text{watt}} \times \frac{10^3 \text{ mV}}{1 \text{ volt}}$$

$$\text{Voltage signal} = 6.3 \times 10^{-3} \text{ mV}$$

This result, like the first calculation of the voltage signal, was too small to observe on the oscilloscope.

It should be pointed out that these calculations were, first, for optimal reflection and minimal loss assumed over conditions and, secondly, neglected losses in the laser beam

after leaving the cavity. Certainly, these optimum reflections and loss conditions were not always present. There were some losses in the output beam due to slight losses in alignment of the detector.

### C. Third Generation Laser

The results obtained with these two laser tube reactors, and the kinetic calculations permit the design of a yet further improved third generation laser reactor assembly.

This third generation laser has to produce a greater amount of excited species  $\text{NO}_2^*$ , at least ten times as much as the second laser tube in order to attain a better detector signal. The excited  $\text{NO}_2^*$  can be increased by increasing the concentrations of NO and  $\text{O}_3$  reactant feeds as shown by Figure 16, (NO conc. vs.  $\text{NO}_{2\text{max}}^*$ ). However, increasing the NO concentration also brought adverse effects due to increased relaxation rates so that the reaction time must be shorter, as shown in Figure 15, (NO conc. vs.  $t_{\text{max}}$ ) or relaxation will stop lasing from occurring. A solution to this problem is a transverse type of laser tube, where the reaction distance is short (only across a tube diameter), as well as the reaction time, but the length (i.e. conc. of  $\text{NO}_2^*$ ) greatly increased. The vacuum pump should also be increased to one of higher capacity for faster flow rates, shorter reaction time. The number of reactant feed inlets are limited to the capacity of the vacuum pump. The reactant feed inlets geometry should also be optimized to have as instantaneous a reaction as possible. A schematic diagram is shown in

Figure 17. Heating the reactor to increase the reaction rate will also help increase the laser's output. The windows are in Brewster's angle for decreased scattering losses.

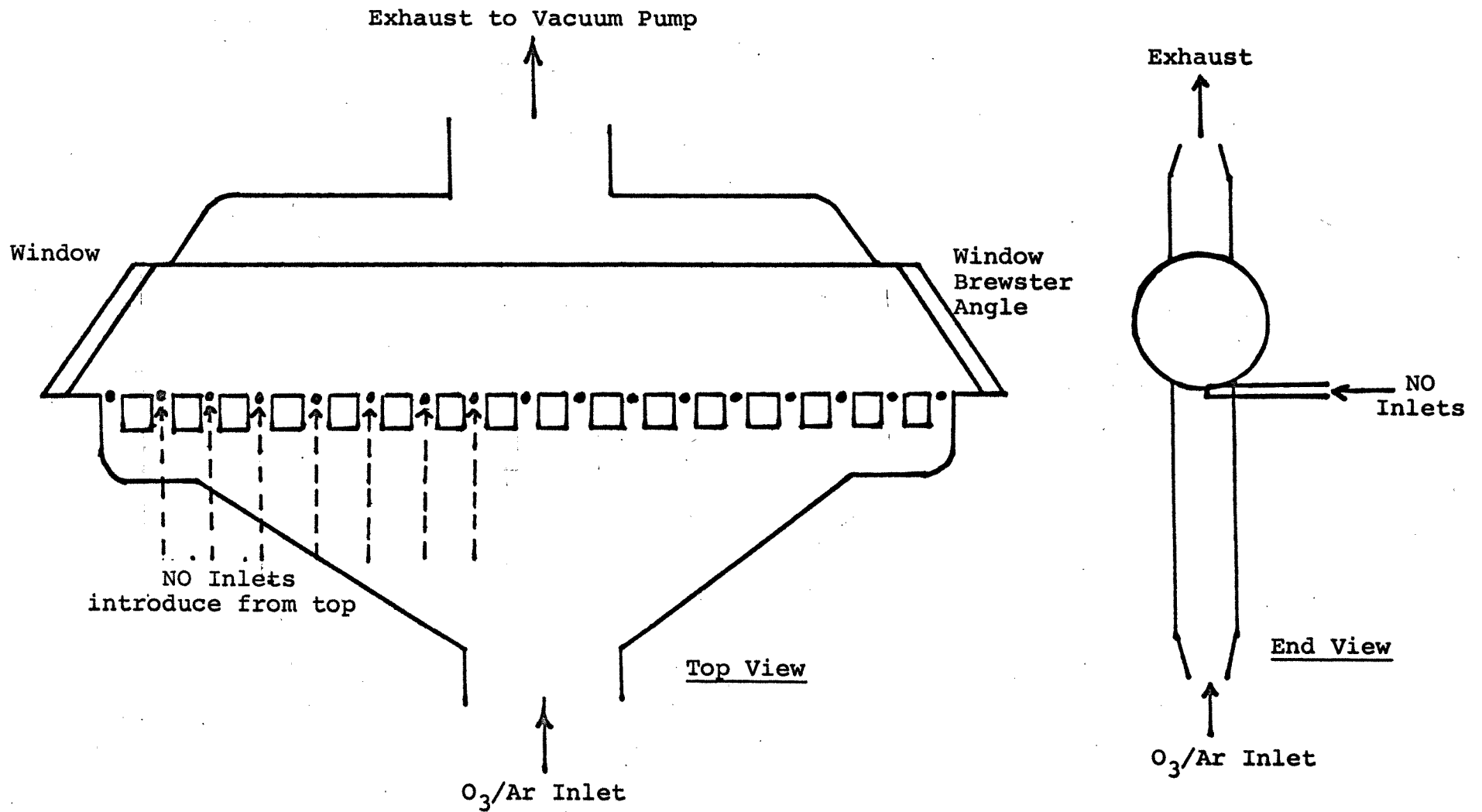


FIGURE 17. Schematic Diagram of the Third Generation Laser Tube

## V. CONCLUSION

The design of a purely chemical laser based on the reaction of  $\text{NO} + \text{O}_3 \rightarrow \text{NO}_2^* + \text{O}_2$  in the vapor phase to produce, instantaneously, and as a principal product vibrationally excited species  $\text{NO}_2^*$  has been attempted. This  $\text{NO}_2^*$  relaxes through collisions and IR emission (3.2 - 3.6  $\mu\text{m}$ ). It was attempted in this study to bring about stimulated emission of the excited  $\text{NO}_2^*$  species thereby inventing a new, purely chemical laser. A series of computer program calculations on the kinetics involved showed support for the formation of the population inversion of the vibrationally excited species,  $\text{NO}_2^*$ . Calculations were also made to optimize the reaction kinetic parameters. The experiments were conducted in two generations of reactor tube systems. The first one, initial laser tube, was 21 cm long by 2 cm ID which did not produce an average population inversion over its length. No lasing could be achieved in this reactor tube. The modified laser tube, which had a shorter reaction distance and time compared to the initial laser tube, showed, through calculations, that a population inversion was achieved and lasing action was therefore attainable. Unfortunately, both reactor tube showed only intermittent, sporadic signals, indications perhaps of weak lasing action which were not reproducible and inconclusive. Calculations of possible power output showed the lasing intensity was projected as being below our detection limit.

Calculations have also shown that higher total numbers of vibrationally excited species in the reactor are required in order to enhance lasing action and to overcome various losses present in the system. This brings about a third generation laser design consisting of a number of transverse flow inlets for the reactants, with similar reaction distance and reaction time as the modified laser tube. This should bring about a significantly larger signal. Extension to a longer, transverse reactor is desirable, provided the vacuum pump capacity will also be increased to accommodate the higher volume flow.



**APPENDIX 1**

```

          $JOB          MALALIS
1          IMPLICIT REAL (A-Z)
2          REAL*8 NO2,NO,NO2M,NO2E,NO2L,O3
-----
          C CONRADO MALALIS KINETICS RUN
          C DATA AND CONDITIONS
3          K1=1.61E-14
4          K2=5.1E-13
5          K3=2.57E-13
6          K4=1.8E-12
7          K5=3.0E-13
8          K6=250
9          K7=1.8E-15
10         O3=2.0E11
11         AR=6.0E16
12         DELT=2.0E-4
13         75 READ(5,110) NO
14         NO2E=0.0
15         NO2L=0.0
16         O2=0.0
17         NO2=0.0
2414.2015 R000 VS/9 REMOTE BATCH MONITORING
18         T=0.0
19         IF(NO.LT.1.0)GO TO 998
20         7 WRITE (6,95)
21         10 NO2M=K1*O3*NO*DELT
22         NO2L=NO2E*(K2*O2+K3*O3+K4*NO+K5*NO2+K6+K7*AR)*DELT
23         NO2E=NO2M-NO2L+NO2E
24         T=T+DELT
          C UPDATE CONCENTRATIONS
25         O2=O2+NO2M
26         O3=O3-NO2M
27         NO=NO-NO2M
28         NO2=NO2+NO2L
29         WRITE(6,100) NO2E,T,NO,O3,NO2
30         IF(T.GT.0.04) GO TO 75
31         IF(NO2E.GT.1.0D46)GO TO 75
32         IF(NO2E.LT.1.0)GO TO 75
33         GO TO 10
34         95 FORMAT('1',5X,' NO2E ',7X,' TIME ',8X,' NO ',10X,' O3O ',
          610X,' NO2G ',//)
35         100 FORMAT(D14.6,E14.6,3D14.6)
36         110 FORMAT(D14.6)
37         998 STOP
38         END

```

\$ENTRY

N02E	TIME	NO	030	N02G
0.322000D 06	0.200000E-03	0.500000D 12	0.200000D 12	0.000000D 00
0.620883D 06	0.400000E-03	0.499999D 12	-0.199999D 12	0.231165D 05
0.898308D 06	0.600000E-03	0.499999D 12	0.199999D 12	0.676898D 05
0.115582D 07	0.800000E-03	0.499999D 12	0.199999D 12	0.132180D 06
0.139484D 07	0.999999E-03	0.499998D 12	0.199998D 12	0.215156D 06
0.161670D 07	0.120000E-02	0.499998D 12	0.199998D 12	0.315292D 06
0.182263D 07	0.140000E-02	0.499998D 12	0.199998D 12	0.431355D 06
0.201378D 07	0.160000E-02	0.499997D 12	0.199997D 12	0.562202D 06
0.219120D 07	0.180000E-02	0.499997D 12	0.199997D 12	0.706772D 06
0.235589D 07	0.200000E-02	0.499997D 12	0.199997D 12	0.864079D 06
0.250875D 07	0.220000E-02	0.499996D 12	0.199996D 12	0.103321D 07
0.265064D 07	0.240000E-02	0.499996D 12	0.199996D 12	0.121331D 07
0.278234D 07	0.260000E-02	0.499996D 12	0.199996D 12	0.140360D 07
0.290459D 07	0.280000E-02	0.499995D 12	0.199996D 12	0.160335D 07
0.301806D 07	0.300000E-02	0.499995D 12	0.199995D 12	0.181187D 07
0.312338D 07	0.320000E-02	0.499995D 12	0.199995D 12	0.202854D 07
0.322114D 07	0.340000E-02	0.499995D 12	0.199995D 12	0.225276D 07
0.331188D 07	0.360000E-02	0.499994D 12	0.199994D 12	0.248401D 07
0.339610D 07	0.380000E-02	0.499994D 12	0.199994D 12	0.272177D 07
0.347428D 07	0.400000E-02	0.499994D 12	0.199994D 12	0.296558D 07
0.354685D 07	0.420000E-02	0.499993D 12	0.199993D 12	0.321500D 07
0.361420D 07	0.440000E-02	0.499993D 12	0.199993D 12	0.346963D 07
0.367672D 07	0.460000E-02	0.499993D 12	0.199993D 12	0.372909D 07
0.373475D 07	0.480000E-02	0.499992D 12	0.199992D 12	0.399305D 07
0.378862D 07	0.500000E-02	0.499992D 12	0.199992D 12	0.426116D 07
0.383861D 07	0.519999E-02	0.499992D 12	0.199992D 12	0.453315D 07
0.388502D 07	0.539999E-02	0.499991D 12	0.199991D 12	0.480873D 07
0.392809D 07	0.559999E-02	0.499991D 12	0.199991D 12	0.508763D 07
0.396807D 07	0.579999E-02	0.499991D 12	0.199991D 12	0.536963D 07
0.400518D 07	0.599999E-02	0.499990D 12	0.199990D 12	0.565450D 07
0.403963D 07	0.619999E-02	0.499990D 12	0.199990D 12	0.594203D 07
0.407160D 07	0.639999E-02	0.499990D 12	0.199990D 12	0.623204D 07
0.410128D 07	0.659999E-02	0.499989D 12	0.199989D 12	0.652434D 07
0.412882D 07	0.679999E-02	0.499989D 12	0.199989D 12	0.681877D 07
0.415439D 07	0.699999E-02	0.499989D 12	0.199989D 12	0.711518D 07
0.417812D 07	0.719999E-02	0.499988D 12	0.199988D 12	0.741343D 07
0.420014D 07	0.739999E-02	0.499988D 12	0.199988D 12	0.771337D 07
0.422059D 07	0.759999E-02	0.499988D 12	0.199988D 12	0.801490D 07
0.423956D 07	0.779999E-02	0.499987D 12	0.199987D 12	0.831790D 07
0.425717D 07	0.799999E-02	0.499987D 12	0.199987D 12	0.862226D 07
0.427352D 07	0.819999E-02	0.499987D 12	0.199987D 12	0.892788D 07
0.428869D 07	0.839999E-02	0.499986D 12	0.199986D 12	0.923468D 07
0.430278D 07	0.859999E-02	0.499986D 12	0.199986D 12	0.954257D 07
0.431585D 07	0.879999E-02	0.499986D 12	0.199986D 12	0.985146D 07
0.432798D 07	0.899999E-02	0.499986D 12	0.199986D 12	0.101613D 08
0.433924D 07	0.919999E-02	0.499985D 12	0.199985D 12	0.104720D 08
0.434969D 07	0.939999E-02	0.499985D 12	0.199985D 12	0.107835D 08
0.435939D 07	0.959999E-02	0.499985D 12	0.199985D 12	0.110958D 08
0.436840D 07	0.979999E-02	0.499984D 12	0.199984D 12	0.114088D 08
0.437675D 07	0.999999E-02	0.499984D 12	0.199984D 12	0.117224D 08
0.438451D 07	0.102000E-01	0.499984D 12	0.199984D 12	0.120366D 08
0.439171D 07	0.104000E-01	0.499983D 12	0.199983D 12	0.123513D 08
0.439839D 07	0.106000E-01	0.499983D 12	0.199983D 12	0.126666D 08
0.440459D 07	0.108000E-01	0.499983D 12	0.199983D 12	0.129824D 08
0.441034D 07	0.110000E-01	0.499982D 12	0.199982D 12	0.132986D 08

0.441568D 07	0.112000E-01	0.499982D 12	0.199982D 12	0.136800
0.442064D 07	0.114000E-01	0.499982D 12	0.199982D 12	0.139800
0.442524D 07	0.116000E-01	0.499981D 12	0.199981D 12	0.142800
0.442951D 07	0.118000E-01	0.499981D 12	0.199981D 12	0.145800
0.443347D 07	0.120000E-01	0.499981D 12	0.199981D 12	0.148800
0.443714D 07	0.122000E-01	0.499980D 12	0.199980D 12	0.152800
0.444056D 07	0.124000E-01	0.499980D 12	0.199980D 12	0.155800
0.444372D 07	0.126000E-01	0.499980D 12	0.199980D 12	0.158800
0.444666D 07	0.128000E-01	0.499979D 12	0.199979D 12	0.161800
0.444939D 07	0.130000E-01	0.499979D 12	0.199979D 12	0.164800
0.445192D 07	0.132000E-01	0.499979D 12	0.199979D 12	0.167800
0.445427D 07	0.134000E-01	0.499978D 12	0.199978D 12	0.171800
0.445644D 07	0.136000E-01	0.499978D 12	0.199978D 12	0.174800
0.445846D 07	0.138000E-01	0.499978D 12	0.199978D 12	0.177800
0.446034D 07	0.140000E-01	0.499977D 12	0.199977D 12	0.180780
0.446208D 07	0.142000E-01	0.499977D 12	0.199977D 12	0.183980
0.446370D 07	0.144000E-01	0.499977D 12	0.199977D 12	0.187180
0.446519D 07	0.146000E-01	0.499976D 12	0.199977D 12	0.190380
0.446658D 07	0.148000E-01	0.499976D 12	0.199976D 12	0.193580
0.446787D 07	0.150000E-01	0.499976D 12	0.199976D 12	0.196880
0.446907D 07	0.152000E-01	0.499976D 12	0.199976D 12	0.200080
0.447018D 07	0.154000E-01	0.499975D 12	0.199975D 12	0.203280
0.447121D 07	0.156000E-01	0.499975D 12	0.199975D 12	0.206480
0.447216D 07	0.158000E-01	0.499975D 12	0.199975D 12	0.209680
0.447305D 07	0.160000E-01	0.499974D 12	0.199974D 12	0.212880
0.447387D 07	0.162000E-01	0.499974D 12	0.199974D 12	0.216080
0.447463D 07	0.164000E-01	0.499974D 12	0.199974D 12	0.219280
0.447533D 07	0.166000E-01	0.499973D 12	0.199973D 12	0.222480
0.447599D 07	0.168000E-01	0.499973D 12	0.199973D 12	0.225680
0.447659D 07	0.170000E-01	0.499973D 12	0.199973D 12	0.228980
0.447716D 07	0.172000E-01	0.499972D 12	0.199972D 12	0.232180
0.447768D 07	0.174000E-01	0.499972D 12	0.199972D 12	0.235380
0.447816D 07	0.176000E-01	0.499972D 12	0.199972D 12	0.238580
0.447861D 07	0.178000E-01	0.499971D 12	0.199971D 12	0.241780
0.447902D 07	0.180000E-01	0.499971D 12	0.199971D 12	0.244980
0.447941D 07	0.182000E-01	0.499971D 12	0.199971D 12	0.248180
0.447976D 07	0.184000E-01	0.499970D 12	0.199970D 12	0.251480
0.448009D 07	0.186000E-01	0.499970D 12	0.199970D 12	0.254680
0.448040D 07	0.188000E-01	0.499970D 12	0.199970D 12	0.257840
0.448068D 07	0.190000E-01	0.499969D 12	0.199969D 12	0.261060
0.448094D 07	0.192000E-01	0.499969D 12	0.199969D 12	0.264270
0.448119D 07	0.194000E-01	0.499969D 12	0.199969D 12	0.267490
0.448141D 07	0.196000E-01	0.499968D 12	0.199968D 12	0.270710
0.448162D 07	0.198000E-01	0.499968D 12	0.199968D 12	0.273920
0.448181D 07	0.200000E-01	0.499968D 12	0.199968D 12	0.277140
0.448199D 07	0.202000E-01	0.499967D 12	0.199967D 12	0.280360
0.448215D 07	0.204000E-01	0.499967D 12	0.199967D 12	0.283580
0.448230D 07	0.206000E-01	0.499967D 12	0.199967D 12	0.286790
0.448244D 07	0.208000E-01	0.499967D 12	0.199967D 12	0.290010
0.448257D 07	0.210000E-01	0.499966D 12	0.199966D 12	0.293230
0.448269D 07	0.212000E-01	0.499966D 12	0.199966D 12	0.296450
0.448280D 07	0.214000E-01	0.499966D 12	0.199966D 12	0.299670
0.448290D 07	0.216000E-01	0.499965D 12	0.199965D 12	0.302890
0.448299D 07	0.218000E-01	0.499965D 12	0.199965D 12	0.306100
0.448308D 07	0.220000E-01	0.499965D 12	0.199965D 12	0.309320
0.448316D 07	0.222000E-01	0.499964D 12	0.199964D 12	0.312540
0.448323D 07	0.224000E-01	0.499964D 12	0.199964D 12	0.315760
0.448330D 07	0.226000E-01	0.499964D 12	0.199964D 12	0.318980

### SELECTED BIBLIOGRAPHY

- [1] O'Shea, Callen, Rhodes, An Introduction to Lasers and Their Applications. Reading, Mass.: Addison Wesley, 1977, pp. 5-47.
- [2] Ready, John F., Industrial Applications of Lasers. New York: Academic Press, Inc., 1978, p. 25.
- [3] Ready, John F., Industrial Applications of Lasers. New York: Academic Press, Inc., 1978, pp. 138-140.
- [4] Cool, T.A. and Stephens, R.R., "Chemical Laser by Fluid Mixing," Journal of Chemical Physics, vol. 51, 1969, pp. 5175-5176.
- [5] Cool, T.A. and Stephens, R.R., "Efficient Purely Chemical CW Laser Operation," Applied Physics Letters, vol. 16, No. 2, 15 Jan. 1970, pp. 55-58.
- [6] Arnold, S.J., Foster, K.D., Snelling, D.R. and Suart, R.D., "A Purely Chemical HCl Laser," Applied Physics Letters, vol. 30, No. 12, 15 June 1977, pp. 637-639.
- [7] Arnold, S.J. and Foster, K.D., "A Purely Chemical HBr Laser," Applied Physics Letters, vol. 33, No. 8, 15 October 1978, pp. 716-717.
- [8] Richardons, R.J., Ageno, H.Y., Lilenfeld, H.V., Menne, T.J., Smith, J.A. and Wiswall, C.E., "CO Chemical Laser Utilizing Combustor-Generated Reactants," Journal Applied Physics, vol. 50, No. 12, Dec., 1979, pp. 7939-7947.
- [9] Maglotte, D.H., Palonyi, J.C. and Woodall, K.B., "Energy Distribution Among Reaction Products. IV. X + HY (X  $\equiv$  Cl, Br; Y  $\equiv$  Br, I), Cl + DI," Journal of Chemical Physics, vol. 57, No. 4, 15 Aug. 1972, pp. 1547-1560.
- [10] Arnold, S.J., Foster, K.D., Snelling, D.R. and Suart, R.D., DREV Technical Reports, DREV R-4015/75, R-4059/76, R-4060/76, R-4071/76 (DREV: Defense Research Establishment Valcartier). Address: P.O. Box 880 Courcellette, P.Q., Canada.
- [11] Richardson, R.J. and Wiswall, C.E., "Combustor-Driven CO Chemical Laser," Applied Physics Letters, vol. 33, No. 4, 15 Aug. 1978, pp. 296-298.
- [12] Slagle, I.R., Gilbert, J.R. and Gutman, D., "Kinetics of the Reaction Between Oxygen Atom and Carbon Disulfide," Journal of Chemical Physics, vol. 61, No. 2, 15 July 1974, pp. 704-709.

- [13] Lilienfeld, H.V. and Richardson, R.J., "Temperature Dependence of the Rate Constant for the Reaction Between Carbon Monosulfide and Atomic Oxygen," Journal of Chemical Physics, vol. 67, No. 9, 1 Nov. 1977, pp. 3991-3997.
- [14] Clyne, M.A.A., Thrush, B.A. and Wayne, R.P., "Kinetics of the Chemiluminescent Reaction Between Nitric Oxide and Ozone," Transactions Faraday Society, vol. 60, 1964, pp. 359-370.
- [15] Clough, P.N. and Thrush, B.A., "Mechanism of Chemiluminescent Reaction Between Nitric Oxide and Ozone," Transaction Faraday Society, vol. 63, 1967, p. 915.
- [16] Fontyn, A., Meyer, C.B. and Schiff, H.I., "Absolute Quantum Yield Measurements of the NO-O Reaction and its Use as a Standard for Chemiluminescent Reactions," Journal of Chemical Physics, vol. 40, No. 1, Jan. 1, 1964, pp. 64-70.
- [17] Clough, P.N. and Thrush, B.A., "Vibrational Emission by NO<sub>2</sub> in Reaction of Nitric Oxide with Ozone," Transaction Faraday Society, vol. 65, 1969, pp. 23-31.
- [18] Golde, M.F. and Kaufman, F., "Vibrational Emission of NO<sub>2</sub> from the Reaction of NO with O<sub>3</sub>," Chemical Physics Letters, vol. 29, No. 4, 15 Dec. 1974, pp. 480-485.
- [19] Bar-Ziv, E., Moy, J. and Gordon, R.J., "Temperature Dependence of the Laser-Enhanced Reaction NO + O<sub>3</sub> (001) II. Contribution From Reactive and Non-Reactive Channels," Journal of Chemical Physics, vol. 68, No. 3, 1 Feb. 1978, pp. 1013-1021.
- [20] Hui, Kin-Kwak and Cool, T.A., "Experiments Concerning the Laser-Enhanced Reaction Between Vibrationally Excited O<sub>3</sub> and NO," Journal of Chemical Physics, vol. 68, No. 3, 1 Feb. 1978, pp. 1022-1037.
- [21] O'Shea, Callen, Rhodes, An Introduction to Lasers and Their Applications. Reading, Mass.: Addison Wesley, 1977, pp. 73-76.
- [22] Leco Corporation, Tem-Pres Division, 1526 William St., State College, Pennsylvania 16801.
- [23] International Crystal Laboratories, 107 Trumbull St., Elizabeth, N.J. 07206.
- [24] Cotton, F.A. and Wilkinson, G., Advanced Inorganic Chemistry, 2nd Edition. New York, London, Sydney: Interscience Publishers, 1967, p. 345.

- [25] Herzberg, G., Molecular Spectra and Molecular Structure II. Infrared and Raman Spectra of Polyatomic Molecules. New York: Van Nostrand Reinhold Company, 1944, p. 284.
- [26] Herzberg, G., Molecular Spectra and Molecular Structure II. Infrared and Raman Spectra of Polyatomic Molecules. New York: Van Nostrand Reinhold Company, 1944, p. 78.
- [27] Stan, A.T. and Kennedy, J.P., "Infrared Chemiluminescence and Vibraluminescence in the NO-O-NO<sub>2</sub> Reaction System," Journal de Chimie Physique et de Physicochimie Biologique, vol. 64, 1967, p. 124-128.
- [28] Hampson, et al., Review, Chemical Kinetic and Photochemical Data for Modeling Atmospheric Chemistry, NBS, Technical Note 866, 1973, p. 28.
- [29] Birks, J.W., Shoemaker, B., Leek, T.J. and Hinton, D.M., "Studies of Reactions of Importance in the Stratosphere. I. Reaction of Nitric Oxide with Ozone," Journal of Chemical Physics, vol. 65, No. 12, 15 Dec. 1976, pp. 5181-5185.
- [30] Bien, Fritz, "Measurements of the Nitric Oxide Ion Vibrational Absorption Coefficient and Vibrational Transfer to N<sub>2</sub>," Journal of Chemical Physics, vol. 69, No. 6, 15 Sept. 1978, pp. 2631-2638.
- [31] Levron, D. and Phelps, A.V., Quenching of N<sub>2</sub> ( $A^3\Sigma_u^+$ ,  $V = 0,1$ ) by N<sub>2</sub>, Ar and H<sub>2</sub>," Journal of Chemical Physics, vol. 69, No. 5, 1 Sept. 1978, pp. 2260-2262.
- [32] Hovis, F.E. and Moore, C.B., "Vibrational Relaxation of NH<sub>3</sub>( $\nu_2$ )," Journal of Chemical Physics, vol. 69, No. 11, 1 Dec. 1978, pp. 4947-4950.
- [33] Ready, John F., Industrial Applications of Lasers. New York: Academic Press, Inc., 1978, pp. 19-22.
- [34] O'Shea, Callen, Rhodes, An Introduction to Lasers and Their Applications. Reading, Mass.: Addison Wesley, 1977, p. 12.
- [35] Frost, A.A. and Pearson, R.G., Kinetics and Mechanism. New York: John Wiley & Sons, Inc., 1953, pp. 1-14.